Research Square

Preprints are preliminary reports that have not undergone peer review.
They should not be considered conclusive, used to inform clinical practice,
or referenced by the media as validated information.

Mechanical and early age performance of CO2 mineralized recycled fines from real waste stream sources compared to low calcium blends with traditional SCMs

Juan Manuel Etcheverry

juanmanuel.etcheverry@ugent.be

Ghent University

Nele De Belie

Ghent University

Research Article

Keywords:

Posted Date: November 13th, 2026

DOI: https://doi.org/10.21203/rs.3.rs-11443410/v1

License: This work is licensed under a Creative Commons Attribution 4.0 International License.
Read Full License

Additional Declarations:
No competing interests reported.

Figure 10 is not available with this version

Mechanical and early age performance of CO_2 mineralized recycled fines from real waste stream sources compared to low calcium blends with traditional SCMs

Juan Manuel Etcheverry [1], Nele De Belie [1]

[1] Magnel-Vandepitte Laboratory for Structural Engineering and Building Materials, Ghent University, Technologiepark Zwijnaarde 60, 9052 Ghent, Belgium

Abstract

The declining availability of traditional supplementary cementitious materials (SCMs) has increased interest in alternative low-carbon binder constituents. This study evaluates CO_2-mineralized recycled fines obtained from three construction and demolition waste streams as clinker replacement in binders containing 30% Portland cement and 70% SCMs. Mineralization increased calcium carbonate content and improved the reactivity of the recycled fines.

The materials were investigated using calorimetry, thermogravimetric analysis, porosity measurements, and compressive strength testing on mortar bars. Compared with untreated recycled fines, mineralized materials showed greater early-age reactivity, resulting in higher heat release and calcium hydroxide consumption after calorimetry. They also refined pore structure by reducing threshold pore size.

Mortars containing 70% mineralized recycled concrete fines achieved higher 28-day strength than blends containing natural pozzolan with limestone and performed similarly to limestone-calcined clay systems with the same clinker content. Environmental assessment indicated a favorable balance between strength and carbon emissions, particularly when accounting for carbon dioxide uptake during mineralization.

Introduction

Concrete is the most widely used construction material in the world. This extensive use is driven by its relatively low cost, good mechanical performance, durability and adaptability to a wide range of applications. As a consequence, the vast production of concrete, and particularly cement, is associated with significant environmental impacts. As demand for infrastructure continues to grow, especially in developing regions, reducing the carbon footprint of concrete has become a major challenge for both industry and researchers [1]. One of the main strategies has been the replacement of clinker with supplementary cementitious materials (SCMs) [2]. The availability of conventional SCMs, such as fly ash and blast furnace slag (S) is expected to decline in the coming decades. This is reflected in the EU-27, where the use of CEM III (slag-based cement) has consistently represented only about 10% of cement use over the last 20 years [3], despite clinker replacement levels of up to 90% being technically feasible in CEM III/C in EN 197-

1:2011 standard. Consequently, alternative SCMs that are locally available and can be produced in large quantities are needed to further reduce the environmental impact of cement production [4].

Recycled concrete fines (RCFs), generated during the processing of construction and demolition waste (CDW), represent a promising option because substantial quantities are produced every year, while a large proportion still ends up in low-value applications or disposal. CDW represents one of the most significant waste streams in the European Union. In 2018, economic activities and households across the EU generated more than 2.3 billion tonnes of waste, with the construction industry accounting for more than one-third of this total [5]. When mineral waste originating from mining and quarrying activities is included, mineral-based materials constitute nearly two-thirds of all waste produced. Excluding excavated soils, CDW is composed of a diverse mixture of materials, including concrete, masonry products, gypsum, timber, glass, metals, plastics, and other construction-related residues [6]. As concrete typically represents a substantial share of this waste stream, it offers considerable opportunities for recycling and resource recovery within a circular construction economy. Recent studies have shown that, after CO_2 mineralization, these fines can be transformed into reactive cementitious materials capable of partially replacing clinker while permanently storing captured carbon. Their use would not only reduce emissions associated with cement consumption but also strengthen local supply chains. New SCMs decrease reliance on increasingly scarce industrial by-products, and support a more circular construction sector in densely populated regions of the world, where demolition is often needed before new construction takes place [4].

Existing literature addresses the CO_2 mineralization process of recycled fines obtained mostly from laboratory-made cement paste with short curing times (weeks). Some studies have tackled this issue by using cement paste with high degrees of reaction, which would lead to similar observations than in mixes after service life in perfect recycling conditions and obtained via advanced sorting techniques [7], [8], [9], [10], [11]. However, the material available for CO_2 mineralization is the one obtained from crushing existing concrete that may already contain impurities (rubble) or has gone through pre-carbonation (either during service life or while located in stocked piles). In addition, most of the recycled fines are obtained as leftovers of the primary crushing process that has the objective of obtaining coarse recycled aggregates (> 4mm fractions) for the production of new concrete. In the remaining recycled fines, there might still be an important fraction of natural sand which just by the well-known dilution effect may reduce the efficiency of the recycled concrete fines for SCMs production after CO_2 mineralization.

The rationale behind previous studies is that lab-made RFs appear to be promising supplementary cementitious materials providing a faster reactivity than other SCMs commercially available [9]. These findings in blended cements with 60% clinker and 40% carbonated recycled fines suggest a contribution of carbonated RFs 45% higher than for limestone filler in a reference mix made with 60% clinker and 40% limestone filler. In addition, the contribution of 40% RFs to the 28d-compressive strength is up to 20 MPa measured on mortar prisms according to EN 196-1.

The mineralization process of the RFs serves as a tool to accelerate the carbonation process of the materials from lifetime periods under natural exposure conditions to hours in specially developed setups. During this process, the hydrates such as ettringite, calcium hydroxide and C-S-H are disturbed, leading to the formation of calcium carbonate with silicate and aluminate ions trapped within the carbonate grains [9]. The addition of alkalis and sulfates during the mineralization process has also an effect on the resulting phases and the speed of the CO_2 mineralization process [8], [12]. The present study adopts the mineralization setup and conditions proposed in a previous study [9]. The only modification concerns the

treatment of the mineralized samples used for compressive strength testing. Unlike the previous methodology, the samples were not subjected to centrifugation and filtration after mineralization. Instead, the fines were allowed to settle naturally, after which the supernatant was removed. The recovered fines were subsequently dried at 40 °C to remove the remaining water, thereby retaining some of the dissolved ions within the solid SCM matrix. This approach is motivated by the practical challenges associated with centrifuging recycled fines at an industrial scale in a cost-effective manner. Alternatively, residual heat from industrial processes could be utilized to dry the materials efficiently, while minimizing the loss of ions in solution, which may otherwise occur in systems relying on centrifugation. Certainly, the mineralization solution may contain alkalis and sulfates that would have an effect of the hydration and strength development process as explained by us in previous studies [13], [14], which is discussed in the article.

This study specifically focuses on mixes containing high proportions of mineralized recycled (concrete) fines derived from three different waste streams sources for use in low-strength applications, which, to the best of our knowledge, has not been systematically investigated before. This approach was chosen because higher-strength concrete applications are typically marketed with certifications in mature markets, where regulatory frameworks permitting the incorporation of mineralized recycled fines at replacement levels exceeding 29% are not yet available. In fact, most of the mixes evaluated in this study would not fall within the existing categories defined by EN 197-1, EN 197-5 and EN 197-6. Conversely, developing or emerging markets may have the opportunity to adopt performance-based standards; however, they are likely to lack a sufficiently large stock of recycled aggregates (and, consequently, recycled fines) to justify investments in carbon mineralization and CO_2 capture facilities, making the replacement of natural and artificial SCMs with mineralized recycled fines economically feasible [15].

The suitability and sustainability of CO_2-mineralized recycled fines (M-RFs) obtained from real waste streams as constituents of low-clinker blended cements containing 30% Portland cement is assessed. Their performance is benchmarked against a range of commercially available SCM systems, including metakaolin, natural pozzolan, blast furnace slag and CEM I. Particular attention is given to the contribution of M-RFs to early-age hydration, portlandite consumption, pore structure, and compressive strength development under calcium-deficient conditions typical of low-clinker binders. In addition, the ability of a modified version of the R3 test and the conventional ASTM C1897 R3 test to predict the reactivity and strength contribution of mineralized recycled fines is assessed. Finally, the study evaluates whether the replacement of conventional SCMs with M-RFs can provide a favorable balance between mechanical performance and environmental impact, thereby contributing to the development of more circular and resource-efficient cementitious materials.

Materials and Methods

2.1. Materials

Three materials were selected to evaluate in which scenarios CO_2 mineralization of recycled fines contributes to the chemical reactivity and early microstructural development of blended cement pastes. Dcon are fines from high-quality recycled concrete; its 4–20 mm fraction is BENOR-certified, exhibiting water absorption values below 5% (24 h). Dmix consists of fines from mixed concrete waste combined with rubble and waste bricks; this fine fraction is primarily used for soil stabilization. LAB are fines obtained by

crushing a waste concrete (laboratory-made and cured for 91 days in wet-room) that is expected to contain unreacted pozzolanic SCMs, specifically modified ferro-silicate slag, as reported by [16]. The concrete contained 390 kg binder/m^3, of which 70% was PC, 30% was non-ferrous slag. It was stored indoors (60% RH and 20 °C) for about 4 years after being wet-cured for 91 days.

The RFs (Dcon, Dmix and LAB) were subjected to CO_2 treatment (mineralization) using a wet process, with the objective of accelerating carbonation and achieving high degree of carbonation, which eventually releases silicon and aluminium ions, thereby enhancing the chemical reactivity of waste recycled fines [11], which would otherwise behave predominantly as inert fillers [17].

A gas mixture consisting of 70% nitrogen and 30% CO_2 was introduced into the treatment solution (0.1 M Na_2SO_4 solution) through a hose equipped with a porous diffuser (solid sponge) capable of generating microbubbles. The diffuser was positioned approximately 2 cm above the bottom of a borosilicate glass beaker. The gas flow rate was maintained at 5 L/h per 1.0g of fines. About 10g of recycled fines were then added into a 100g sodium sulfate solution. The suspension was continuously stirred by a magnetic stirrer (400 rpm) to ensure homogeneity and uniform distribution of the gas bubbles. The pH and temperature were monitored at 5-minute intervals. The duration of the mineralization was 60 minutes/10g of dry (40 °C) solids. After the mineralization process, the fines were allowed to settle (24h) and the excess of water was removed via vacuum filtration. The remaining fines were dried at 40 °C for 24 hours. For the particular case of thermogravimetric analysis and calorimetry experiments, the mineralized RFs (M-Dcon, M-Dmix and M-LAB) were also washed with isopropanol (2 cycles of 60 minutes) followed by diethyl ether washing, filtration and drying at 40 °C for about 10 minutes to remove the excess of solvent [18]. M-Dcon samples used for compressive strength testing were not subjected to centrifugation and filtration after mineralization. Instead, the fines were allowed to settle naturally, after which the supernatant was collected and the recovered fines were subsequently dried at 40 °C to remove the remaining water.

Cement pastes with high water-to-binder ratio (0.70) were prepared. The use of high water to binder ratios was decided to avoid the use of superplasticizer (with unknown interaction with the mineralized SCMs), facilitate moisture distribution during curing and at the same time minimise that the lack of capillary water [19] may limit the reaction of the CO_2 mineralized materials or SCMs in cement blends. Certainly, a greater porosity than in conventional blended cements with conventional water-to-binder ratios is expected as discussed in the article.

In addition, conventional cements and SCMs were used in this study for comparative purposes. These included Portland cement (PC, CEM I 52.5N; denoted as P in the sample nomenclature), ground granulated blast furnace slag (S), limestone powder (L), trass natural pozzolan (Np) sourced from the Vulkaneifel region, and metakaolin (MK). The metakaolin was characterised by an amorphous content exceeding 70% and a BET specific surface area of 16.0 m^2/g, as reported by the supplier (Xatico).

Table 1 presents the chemical composition (X-ray fluorescence - XRF), density, and particle size distributions (PSDs) of the materials. Particle size distribution was determined using laser diffraction with a Malvern Mastersizer 2000 device. For the case of MK, laser diffraction does not provide reliable PSD and no values for d_v10, d_v50 and d_v90 are reported. In addition to the properties presented in Table 1, in a previous study [17] the bulk density was found to be 800 kg/m^3 for Dcon, 920 kg/m^3 for Dmix and 800 kg/m^3 for LAB and specific surface areas measured via BET analysis were found to be 10.1 m^2/g for Dcon, 8.6 m^2/g for Dmix and 9.8 m^2/g for LAB.

Gypsum (Gyp) and sodium sulfate (both technical grade, purity > 99%) were added in dry solid form to the mixes or to the mineralization solution, at the dosages specified in Table 2. Table 2 summarizes the mix design for all investigated paste and mortar compositions.

Table 1. Chemical composition (XRF, % m/m), density, and particle size distribution of the materials.

Chemical composition	PC	L	MK	Np	S	Dcon	Dmix	LAB
CaO	64.3	54.7	1.7	17.4	40.8	31.4	11.6	19.8
SiO_2	18.3	1.5	60.4	29.0	33.3	38.8	63.3	49.7
MgO	1.4	0.3	1.0	3.7	7.8	-	-	-
Al_2O_3	5.2	0.5	28.8	7.0	12.3	4.0	6.7	5.8
Fe_2O_3	4.0	0.6	4.8	26.9	0.4	2.0	2.5	4.0
Mn_2O_3	-	< 0.1	-	0.2	0.4	-	-	-
Cl	0.06	0.08	0.2	-	-	-	-	-
BaO	-	-	-	-	0.3	-	-	-
SO_3	3.5	0.1	0.3	0.2	2.3	-	-	-
Na_2O	0.2	-	-	1.2	0.4	-	-	-
K_2O	0.4	0.2	0.7	2.8	0.7	-	-	-
TiO_2	-	<0.1	1.8	2.7	2.3	-	-	-
LOI (%)	2.3	42.9	-	-	-	19.7	11.5	16.5
Physical properties								
PSD (μm) $d_v10/d_v50/d_v90$	2.3/10.8/29.4	1.9/6.6/30.2	-	6.4/16.4/38.2	1.3/7.6/26.8	5.0/31.1/77.6	5.2/34.1/74.0	6.9/43.8/97.3
Density (g/cm^3)	3.16	2.69	2.58	2.75	2.89	2.37	2.57	2.49

Table 2. Mix design (mass%) of the studied paste mixtures. The number following the hyphen in the sample designation indicates the Portland cement content. Additionally, for some mixtures, the value shown in parentheses denotes the SCM-to-calcium carbonate ratio.

Designation	PC	L	MK	Np	S	M-Dcon	M-Dmix	M-LAB	Dcon	Dmix	LAB	Gyp/B	W/B
PL-30	30	70	-	-	-	-	-	-	-	-	-	0.035	0.70
PL-30/2.5Gyp	30	70	-	-	-	-	-	-	-	-	-	0.025	0.70
LC3-30 (1:1)	30	35	35	-	-	-	-	-	-	-	-	0.060	0.70
LC3-30 (2:1)	30	23	47	-	-	-	-	-	-	-	-	0.080	0.70
PS-30	30	-	-	-	70	-	-	-	-	-	-	0.035	0.70
PLNp-30 (1:1)	30	35	-	35	-	-	-	-	-	-	-	0.035	0.70
PM-Dcon-30	30	-	-	-	-	70	-	-	-	-	-	0.035	0.70
PDcon-30	30	-	-	-	-	-	-	-	70	-	-	0.035	0.70
PM-Dmix-30	30	-	-	-	-	-	70	-	-	-	-	0.035	0.70
PDmix-30	30	-	-	-	-	-	-	-	-	70	-	0.035	0.70
PM-LAB-30	30	-	-	-	-	-	-	70	-	-	-	0.035	0.70
PLAB-30	30	-	-	-	-	-	-	-	-	-	70	0.035	0.70
LC3-50 (2:1)	50	20	30	-	-	-	-	-	-	-	-	0.050	0.70
CEM I	100	-	-	-	-	-	-	-	-	-	-	-	0.70

2.2. Modified reactivity test

A modified version of the R^3 test [20], suitable for assessing both the extent and nature of SCM reactivity, was employed using isothermal calorimetry followed by TGA. Prior to testing, all materials were preconditioned at 50 °C for 24 h to ensure thermal equilibrium. The SCMs were combined with calcium hydroxide at a mass ratio of 1:3 and subsequently mixed with a 0.5 M KOH solution, using a liquid-to-solid ratio of 0.9. This alkaline environment promotes the dissolution and reaction of the SCMs under controlled and reproducible conditions that would not be possible due to the different reactivity of Portland cements commercially available. Samples for this test received two different mixing procedures: a) manual mixing [20] for 2 minutes inside calorimetry vials (15g paste) and b) external mechanical high speed-mechanical (1600 rpm) mixing for 2 minutes (100g paste). About 15g of the resulting pastes were transferred into sealed ampoules suitable for isothermal calorimetry, minimizing exposure to ambient conditions and preventing moisture loss. The samples were then subjected to calorimetric testing at a constant temperature of 50 °C for a total duration of 10 days, during which heat evolution was continuously monitored.

Upon completion of the calorimetric measurements (10d), the ampoules were opened, and the hydrated pastes were extracted. To stop further hydration and remove residual pore solution, the samples were solvent-exchanged using isopropanol. The treated pastes were then dispersed onto Petri dishes and dried in a ventilated oven at 40 °C for 30 minutes to eliminate remaining solvent without inducing thermal alteration of hydration products. The dried materials were gently ground, collected as powders, and stored in airtight plastic containers that were kept under light vacuum to prevent carbonation prior to TGA, which was conducted as described in subsequent sections.

2.3. ASTM reactivity test

The conventional version of the R^3 test, suitable for assessing the chemical reactivity of SCMs, was employed using isothermal calorimetry according to ASTM C1897. Prior to testing, all materials were preconditioned at 40 °C for 24 h to ensure thermal equilibrium. The SCMs were combined with calcium hydroxide at a mass ratio of 1:3 and subsequently mixed with a potassium sulfate and potassium hydroxide solution. In addition, minor quantities of calcium carbonate powder were added. Immediately after high speed-mechanical (1600 rpm) mixing for 2 minutes, the resulting pastes were transferred into sealed ampoules suitable for isothermal calorimetry. The mass of paste within the ampoules was about 15 g. The samples were then subjected to calorimetric testing at a constant temperature of 40 °C for a total duration of 7 days, during which heat evolution was continuously monitored.

The highly alkaline environment employed in the R^3 test promotes the dissolution and subsequent reaction of SCMs under controlled and reproducible conditions, mitigating the variability typically associated with the use of commercially available Portland cements, whose compositional and reactivity differences can significantly influence hydration behavior. Compared to modified version of the R^3 test, the present methodology incorporates sulfate and carbonate ions, which play a crucial role in stabilizing dissolved species through precipitation and complexation reactions. The inclusion of these ions also enhances the representativeness of the test conditions, as sulfate and carbonate phases are commonly present in blended cement systems. As a result, the R^3 test (cumulative heat release after 7 days) has previously demonstrated excellent interlaboratory reproducibility and strong correlation ($R^2 > 0.7$) with the 28-day compressive strength of mortar specimens prepared in accordance with NBN EN 196-1:2016, containing 30% SCMs and 70% Portland cement [21].

2.4. Isothermal calorimetry on paste samples

Isothermal calorimetry measurements were performed at 40 °C using a TAM Air calorimeter. Prior to mixing, all solid components and the mixing water were precisely weighed and conditioned at 40 °C for a period of 24 hours. Paste formulations (Table 2) were then prepared by combining demineralized water at a water-to-binder ratio of 0.70 with the dry materials.

Mixing was carried out at 1600 rpm for 2 minutes. Immediately after mixing, a representative portion of approximately 15 g was extracted from the total batch (70 g) using a plastic pipette and placed into a glass ampoule. The ampoule was sealed and inserted into the calorimeter, where heat evolution was continuously monitored over a period of 7 days. After 7 days, the paste from the glass ampoule was tested using thermogravimetric analysis.

2.5. Thermogravimetric analysis

Samples were ground to powder using mortar and pestle, and hydration was stopped by two cycles of immersion in isopropanol (1h each) followed by filtration to remove the excess of solvent [18]. Powders were then stored in light vacuum (<0.1 bar) for a maximum period of time of 7 days, during which TGA was performed in a Netzsch STA 449 Jupiter TGA-DTA Analyzer. The temperature ranged from 20 to 1100 °C at a heating rate of 10 °C/min in an inert nitrogen atmosphere. About 50 mg of sample was used in TGA experiments. The tangential method described in [22] was adopted for the quantification of portlandite and carbonates from TGA curves.

2.6. Mercury Intrusion Porosimetry

MIP was conducted using a Pascal 140/440 Thermo Fisher device on sound samples with particle sizes around 5 mm, obtained from the paste samples hydrated for 7 days inside the isothermal calorimetry device at 40 °C. Possible differences in the critical pore size due to self-desiccation reported by Zunino and Scrivener [37] were evident when blended cements were vacuum dried for 2 days instead of 1 month. The reader is referred to the supporting information file for this comparison in blended cements (Fig. S.1). The samples obtained after calorimetry testing were then pre-conditioned by solvent exchange using isopropanol, as recommended in [38], followed by vacuum drying in a desiccator at -0.2 bar for a month. The objective of this approach, instead of just solvent exchange, was to compare samples in a pessimism scenario. For each measurement, approximately 1.0 g of sample was placed in the dilatometer. Vacuum was applied, followed by the introduction of mercury and the application of a 200 kPa pressure to initiate pre-intrusion in the low-pressure device. Subsequently, the dilatometer was transferred to the high-pressure unit, where the pressure was incrementally raised to 200 MPa while recording the intrusion curve. The threshold pore size was determined, with a mercury contact angle set at 142° and the surface tension of the mercury at 0.48 N/m.

2.7. Carbon footprint estimations

The life cycle assessment (LCA) of the mortar mixes was performed using ISO 14040/44 (2006) methodology. Replacing PC with SCMs is generally accepted to reduce the GWP of the mixes. However, the reactivity of the SCMs and the environmental impacts associated with their production must also be considered, especially at low clinker factors. An environmental performance indicator was used to combine environmental impact (GWP) and mechanical performance. This indicator expresses the CO_2 equivalent

emissions per m^3 of mortar required to achieve 1 MPa of compressive strength at 28 days, given that compressive strength at 28 days is the most widely used design parameter.

The CO_2 indicator was calculated on a cradle-to-gate basis for 1 m^3 of mortar. The assessment includes all intermediate processing steps required for Dcon, MK, L, PC, Np, and S. Environmental impacts were regionalized using the current Belgian electricity and fuel mixes, as reported in [23]. Dcon was considered a waste material; therefore, no environmental burdens were allocated to its generation (demolition phase). However, the impacts associated with primary crushing, classification, and secondary crushing operations were included in the assessment [24]. A conservative transportation distance of 100 km was assumed for processing and distribution. For M-Dcon, two scenarios were evaluated. In the first scenario, no credit was assigned for the CO_2 captured during treatment. In the second scenario, the amount of CO_2 bound during mineralization was subtracted from the total emissions. Real field data regarding energy used during mineralization and possible leakage of CO_2 during materials handling are currently not available. Consequently, although this process should be considered in a comprehensive life cycle assessment, it was excluded from the present carbon footprint estimations because of insufficient data.

Although the environmental impacts associated with the production of other SCMs may vary depending on location, raw material availability, and production processes, this study adopted production data for MK and L from Pillai et al. [25], and production data for PC and S from [13], as summarized in Table S.1.- supporting information file. Processing steps required to produce S include granulation, drying, and grinding. In addition, an economic allocation approach based on previous work by the authors was applied [13], whereby 0.84% of the environmental impacts associated with the steelmaking process were allocated to S production [26]. For Np, the environmental burdens associated with extraction, primary crushing, classification, and milling were included in the assessment. Transportation was modelled by truck, resulting in emissions of 0.015 kg CO_2 eq/kg Np (200 km). This assumption is consistent with the fact that 80% of cement transportation within the EU-27 is carried out by truck [27].

2.8. Mechanical strength

Compressive strength tests (three replicates) were performed on (4 × 4 × 16) cm^3 mortar prisms cast in accordance with EN 196-1, using a water-to-binder (w/b) ratio of 0.50 and a sand-to-binder ratio of 3. The mixes evaluated for strength development are summarized in Table 3. After 24 h of curing at >95% relative humidity and 20 °C, a subset of specimens was demolded and tested at 1 day. The remaining specimens were stored at >95% relative humidity and 20 °C until testing at 2, 7, 28 and 180 days. Compressive strength was determined in accordance with EN 196-1. The SCM activity index (AI) is calculated using Equation (1), where CSBCt represents the compressive strength of the blended cement containing the SCM at time t, CSPLt denotes the compressive strength of the Portland limestone cement at the same age, and SCM% corresponds to the mass fraction of SCM in the blended cement. For instance, in PS-30, SCM%=0.70, whereas in the case of LC3-30 (1:1), SCM%=0.35. $CaCO_3$ is not considered as reactive SCM in the denominator.

$$AI = \frac{CSBCt - CSPLt}{SCM\%} \quad \text{Eq. (1)}$$

Table 3. Mortar mixes evaluated via compressive strength and AI. B stands for binder and comprises PC, L, MK, M-Dcon, Np and S. W stands for water.

Designation	PC	L	MK	M-Dcon	NP	S	Gyp/B	Na_2SO_4/B	Sand/B	W/B

PL-30	30	70	-	-	-	-	0.035	0.00	3	0.50
LC3-30 (1:1)	30	35	35	-	-	-	0.060	0.00	3	0.50
PS-30	30	-	-	-	0	70	0.035	0.00	3	0.50
PLNp-30 (1:1)	30	35	-	-	35	-	0.035	0.00	3	0.50
PM-Dcon-30	30	-	-	70	-	-	0.035	0.00	3	0.50
PL-30 NS	30	70	-	-	-	-	0.000	0.10	3	0.50

3.Results and discussion

3.1. Calcium carbonate and portlandite before and after CO_2 mineralization.

Table 4 shows the bound water content (100–500 °C), portlandite (420–470 °C), and calcium carbonate content (500–850 °C) obtained via TGA analysis of the recycled fines before and after CO_2 mineralization (see Fig. S.2. for the full TGA curves). For all recycled fines, the CO_2 mineralization process consistently increased the $CaCO_3$ content at the expense of chemically bound water in the 100–500 °C range. This behavior is expected and can be attributed to the carbonation of cement hydrates such as ettringite, AFm phases and C-S-H. Full carbonation of these hydrates may have not occurred during storage in the stockpiles due to several reasons, that are not the focus of this study (such as, short storage times, excessive or insufficient humidity, more restricted diffusivity as distance from the surface of the stockpiles increases or thermodynamic constraints at natural CO_2 concentrations) [28], [29]. In any case, these limitations were effectively overcome during the mineralization process which consistently increased the $CaCO_3$ content and thus CO_2 uptake in the recycled fines after treatment.

The lowest potential for CO_2 mineralization, in terms of CO_2 uptake, was observed for DMix, which exhibited only a slight increase in $CaCO_3$ content after treatment. In contrast, M-Dcon and M-LAB showed a nearly twofold increase in $CaCO_3$ content, with approximately 45% and 59% of the samples consisting of $CaCO_3$ after CO_2 mineralization, respectively.

As previously suggested by [17], these recycled fines, obtained from real waste streamlines, rarely contain a measurable amount of portlandite. When quantified via tangential method, Dcon was the only RFs showing minor contents of CH (1.3%). It is worth mentioning that the use of the stepwise method for the quantification of CH would gave values within a range of 1% to 4%, but these are simply overestimations of the quantification method as discussed by [22], [30].

Table 4. Chemically bound water, portlandite (CH), calcium carbonate content and CO_2 uptake in RFs before and after CO_2-mineralization process. NM: Not-measured.

	(g/100g sample at 500 °C)		(g/100g sample at 800 °C)	
	BW within 100-500 °C	CH	$CaCO_3$	CO_2 uptake
Dcon	7.0	1.3	25.2	NM

Dmix	3.3	0.0	18.9	NM
LAB	7.6	0.0	33.3	NM
M-Dcon	4.9	0.0	45.3	8.8
M-Dmix	3.1	0.0	23.8	2.2
M-LAB	5.6	0.0	59.0	11.3

The CO_2 uptake (Table 4) during mineralization is calculated as the difference between $CaCO_3$ after and before treatment multiplied by the molar mass of CO_2 (44 g/mol), divided by the molar mass of $CaCO_3$ (100.1 g/mol). The CO_2 capture becomes 8.8 g CO_2/100g of M-Dcon, 2.2 g CO_2/100g of M-Dmix and 11.3g CO_2/100g of M-LAB. Considering that 1.0g of CH could theoretically bind a maximum of only 0.35g CO_2, it is evident that carbonation of hydrates other than portlandite are the main responsible for the increase of the CO_2 uptake potential.

The presence of remaining bound water within the range 100-500 °C suggests that some minor optimization of the mineralization process might be possible. In addition, the amount of pre-carbonation measured in Dcon, Dmix and LAB seems also significant, which may suggest that better handling and taking actions to avoid carbonation of recycled aggregates from real waste steam in stockpiles may help to increase the accountable CO_2 capture during mineralization.

3.2. Calorimetry (modified R3 test)

Figure 1a shows the heat release of recycled cement paste before and after CO_2 mineralization, evaluated using the modified R3 test [31]. Dcon and Dmix exhibit a steady and limited heat release prior to CO_2 mineralization. Similar observations were reported by [32], where similar recycled fines obtained from real demolition streams, without any mineralization treatment, showed only a limited contribution when used as a cement substitute and limit the Portland cement replacement potential to less than 10% before compromising performance.

In contrast, LAB displays significantly higher chemical reactivity. This difference is explained by the substitution level of CEM I by modified ferro-silicate slag in the original mixes (Mix 2 in [33]), indicating that, even after several years in lab environment, a substantial fraction of non-ferrous slag or PC remain unreacted.

After CO_2 mineralization, all three mineralized recycled fines exhibit rapid early-age reactivity (<12 h), followed by a steady increase in heat release. In all cases, the heat released after 24 h exceeds that of the non-mineralized materials, supporting their potential role as early-age reactivity enhancers in blended cement [9]. After 10 days, the total heat release of M-CEM is significantly lower than that of CEM, likely due to prior hydration and/or carbonation of calcium-rich unreacted phases during the mineralization process. The total reactivity of M-Dmix is slightly lower than that of Dmix, whereas for M-Dcon the reactivity increases by approximately 20 J/g binder.

Figure 2b shows the reactivity of MK, Np, S, and quartz powder (Q). MK and S exhibited the highest reactivity after 10 days and the fastest reaction kinetics. According to the modified R3 test, the mineralized

RFs should achieve a final reactivity similar to that of the Np under investigation, but with a faster heat release at early ages.

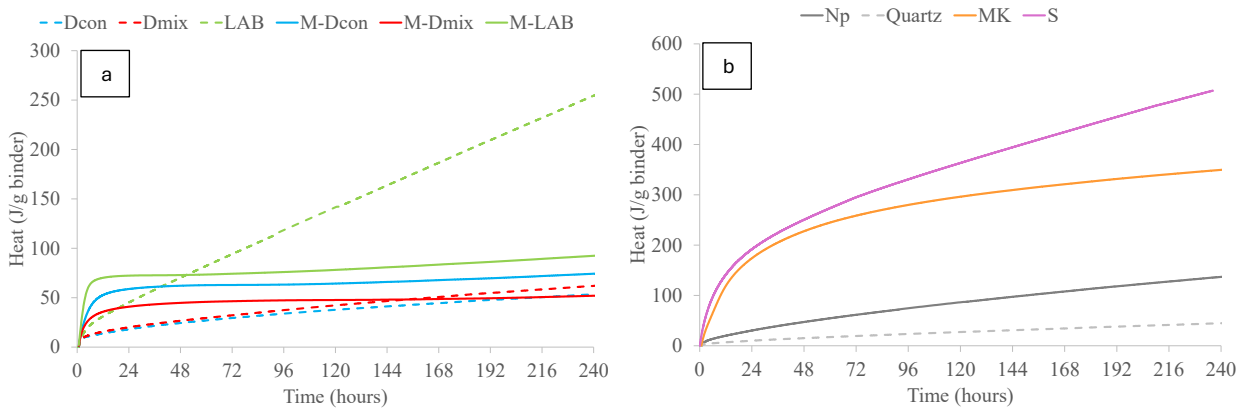


Figure 1. Evolution of heat release by SCMs during modified R3 test (manual mixing) for up to 10 days (50 °C); a) recycled fines before and after mineralization; b) conventional SCMs, such as quartz filler, NP, MK and S.

3.3. Possible limitations of modified R3 reactivity threshold (heat production) in the assessment of recycled fines.

It is important to note that the modified R3 test essentially quantifies both heat production and CH consumption. Based on this method, a reactivity threshold has been proposed, defined by a cumulative heat release of 120 J/g SCM and a CH consumption of 50 g per 100 g SCM at 10 days [34]. For conventional SCMs, dissolution is a prerequisite for their participation in hydrate formation, during which CH is consumed. Certainly, ettringite formation and calcium silicate hydrate formation by pozzolanic reaction release different amounts of heat and also consume different amounts of CH. However, in the case of mineralized RFs, previous studies have shown that the mineralization process may lead to the incorporation of species such as silicates and aluminates within the $CaCO_3$ formed during mineralization [9], [35]. These phases are expected to be thermodynamically unstable and therefore prone to rapid dissolution (closely followed by hydrates precipitation). Consequently, their contribution might not be fully captured by heat release-based reactivity tests due to their rapid dissolution and reprecipitation (when calorimetry involves external mixing), therefore the consumed portlandite measurements proposed by [31] were implemented and also compared to bound water observations.

Figure 2a) shows the poor correlation (for RFs) between the heat release measured via isothermal calorimetry at 10 days with the CH consumption after modified R3 test (for which the CH consumption of a R3 solution with inert quartz filler was taken as reference). As evidenced by the consumption of portlandite after the reactivity test, the reactivity inferred from the heat production during the modified R3 test seems to underestimate the actual potential of mineralized RFs as SCMs. While the reactivity of RFs in terms of heat release is limited compared to other SCMs such as a known highly reactive MK and a low-

reactive Np [31], the CH consumption of the recycled fines (see cluster of M-RFs) is, in fact, greater than the one of Np and about 70% of the reactivity of MK.

Figure 2b) also shows a poor correlation between the heat release measured via isothermal calorimetry at 10 days with the amount of bound water (within the range 20-400 °C) during the modified R3 test for the particular case of M-RFs.

Please, note the importance of including a, per se, non-reactive filler (such as quartz filler) as part of the tested samples, given that even inert fillers give some (limited) heat release and bound water (about 50 J/g SCM and 25 g bound water/100 g of SCM).

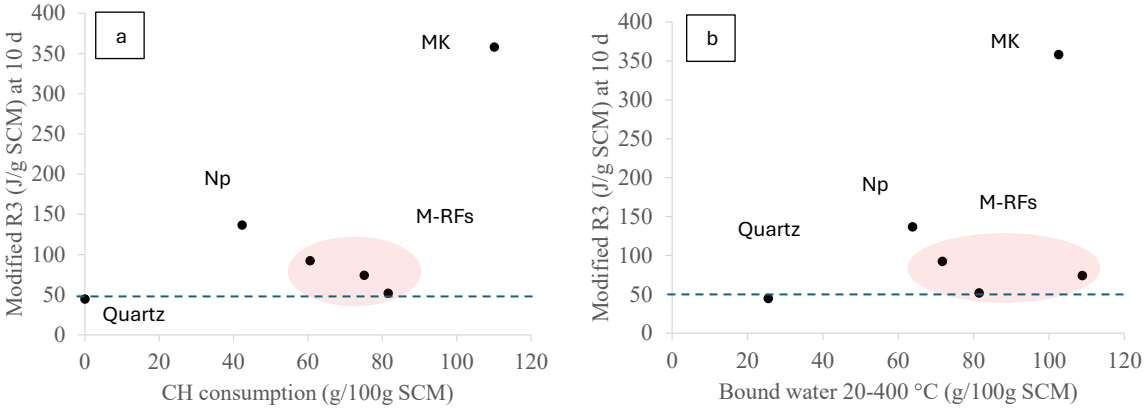


Figure 2. a) Heat released measured via isothermal calorimetry at 10 days versus CH consumption after modified (manual mixing) R3 test (compared to consumption of CH in quartz powder system); and b) heat released measured via isothermal calorimetry at 10 days versus bound water after modified R3 test. The dashed lines represent the heat released at 10 days by inert quartz filler. RFs before mineralization were in the same range as quartz filler.

3.4 Comparison R3 versus modified R3

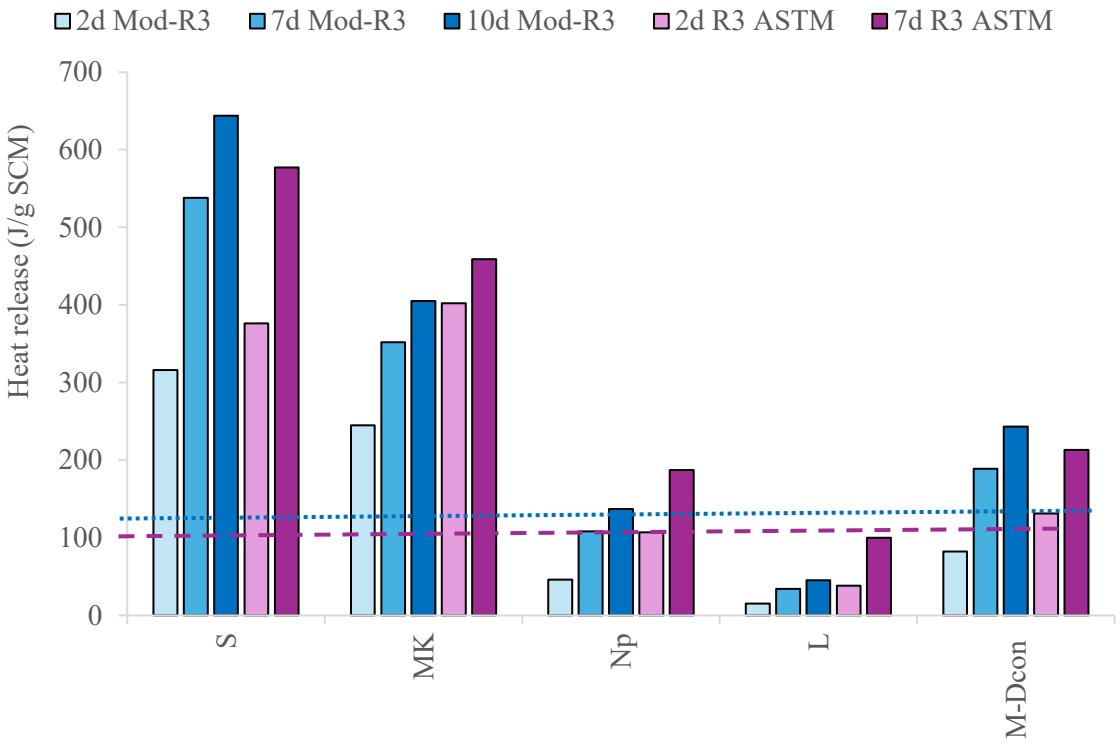


Figure 3. Comparison results of heat release via modified R3 (high-speed mixing) test (2, 7 and 10 days) versus R3 ASTM (2 and 7 days) for S, MK, Np, L and M-Dcon. Dashed line indicates reactivity threshold for ASTM R3 test and dotted line indicates reactivity threshold for modified R3 test.

Figure 3 presents the heat release measured using the R3 (ASTM) and modified R3 test (with high-speed external mixing) procedure for S, MK, Np, L, and M-Dcon. Overall, the R3 ASTM test yields slightly higher heat release values than the modified R3 method at equivalent reaction times, despite the lower testing temperature (40 °C for R3 ASTM versus 50 °C for the modified R3). This outcome appears to indicate that the composition of the modified R3/R3ASTM solution seems to have more influence than the temperature for the SCMs evaluated in this study.

The final reactivity of modified R3 (at 10 days and 50 °C) appears higher than the one of the R3 ASTM (at 7 days and 40 °C) for S and M-Dcon but it remains lower for MK, Np and L. A dedicated study (varying one parameter at the time) may be needed to link such differences to the chemical composition of the SCMs. Within the modified R3 test, the intensity of the mixing process seems to have a measurable effect on heat release at 10 days as well (note the differences in heat release after 10 days for MK, Np and M-Dcon between Fig. 2b and Fig. 3).

In any case, M-Dcon is classified as reactive according to the R3 ASTM threshold (100 J/g SCM) and also according to modified R3 test (if high-speed mixing is used). M-RFs with manual mixing (Fig. 2a) do not seem to pass the modified R3 threshold in terms of heat release. However, CH consumption compared to Q (Fig 2b) in modified R3 with manual mixing still supports the classification [31] of M-Dcon as a low-reactivity pozzolanic material (40–100 g CH/100 g SCM).

3.5. Cumulative heat of hydration on blended cement pastes

Figure 4a illustrates the heat release of conventional mixes, including CEM I, PS-30 (CEM III/B), LC3-50 (2:1), and LC3-30 (1:1), where the MK-to-L ratios are 2:1 and 1:1, respectively. CEM I exhibits the highest heat release at 168h, followed by LC3-50, which is consistent with their high clinker contents compared to systems containing 30% PC. Among the systems containing 30% PC, the contribution of S in PS-30 is approximately 129 J/g of binder relative to the PL-30 reference mix. In LC3-30, the contribution of MK is about 64 J/g of binder compared to the same reference. The contribution of M-Dcon in PM-Dcon-30 is around 37 J/g of binder, while PLNp-30 shows the lowest additional contribution, at approximately 21 J/g of binder.

Figure 4b shows, for pastes containing 30% PC, the contribution of the mineralized recycled fines (M-Dcon, M-Dmix, and M-LAB), which is approximately 40 J/g of binder compared to the PL-30. This contribution occurs predominantly at very early ages (<24 h). This effect is not attributed to a filler effect, but rather to a chemical contribution, likely associated with the rapid dissolution of ions trapped within the calcium carbonate grains during mineralization. This behavior is consistent with the early pozzolanic reaction reported by [9]. Beyond 24 h, only limited additional heat release is observed from the mineralized recycled fines, as the heat evolution curves of all samples become parallel to that of PL-30.

The PL-30 NS mix is intended to demonstrate that, although the presence of sodium sulfate (possibly not fully removed during the filtration of M-Dcon, M-Dmix, or M-LAB after mineralization) can explain the increased rate of heat release (evidenced by the steeper slope compared to PL-30), it does not account for the total contribution of approximately 40 J/g of binder observed for the mineralized materials.

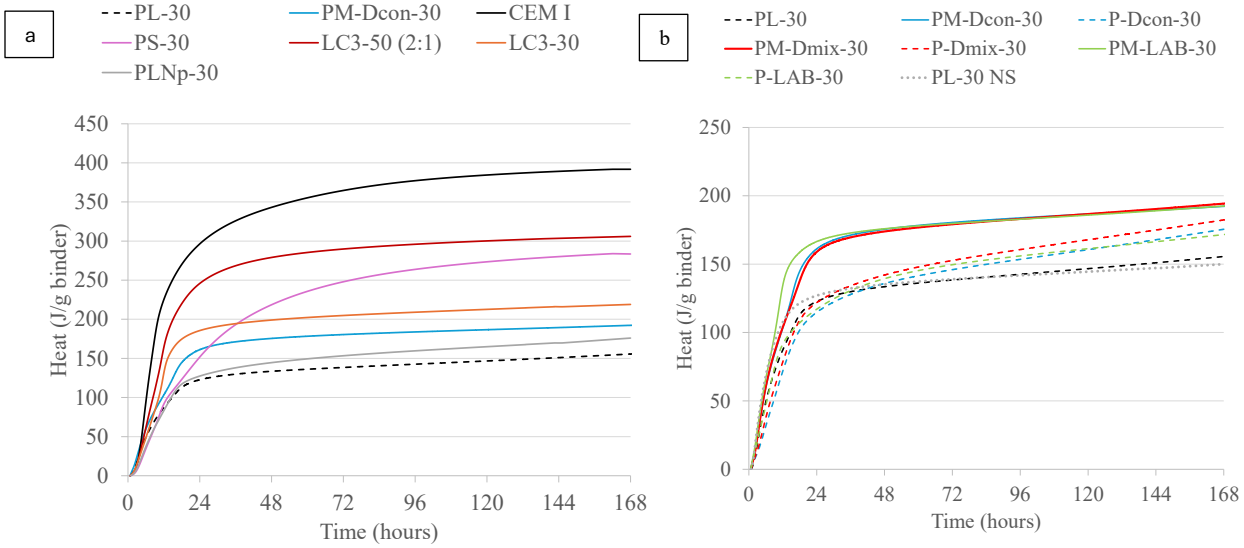


Figure 4. Cumulative heat release measured via isothermal calorimetry for 168h in systems a) containing M-Dcon-30, LAB I, PS-30, LC3-50 (2:1), LC3-30 (1:1) and PLNp-30 (1:1); and b) M-Dcon, M-Dmix,

M-LAB, Dcon, Dmix and LAB. The dashed black line represents the 'baseline' contribution of 30%PC in a system of 30%PC with 70% LL.

3.6. Where does the (early) contribution of mineralized RFs come from?

Heat flow graphs obtained from isothermal calorimetry on cement paste show several distinctive peaks. Properly sulfated systems are characterised by a first peak identified as alite dissolution peak during which C-S-H and CH precipitate, mainly from the dissolution of C_3S. During this period, gypsum is consumed, not only by slow formation of ettringite (due to adsorption of sulfates limiting C_3A dissolution rate) but also by the adsorption of sulfates on the C-S-H. Once gypsum is fully depleted, a sharp peak related to fast formation of ettringite is observed. In some cases, an small hump is observed in between these two main peaks (alite peak and aluminate peak) which was reported to be related to the precipitation of minor amounts of AFm-like phase [19], [36], [37].

Figure 5a shows that the alite dissolution peak is significantly affected by the PC content in the cement blend. This is expected, since with more PC, there is more C_3S (~65% in the CEM I used in this study [14]) available to react. Moreover, the addition of extra sulfate delays the appearance of the aluminate peak, because there is more gypsum to be consumed (PL-30/2.5Gyp versus PL-30 which has 3.5% Gyp). Previous research found that different sources of calcium sulfate may also affect the intensity of the alite peak. It was highlighted that the use of sodium sulfate leads to an increase of the alite peak (by alkalis enhancing dissolution of C_3S and/or more ettringite formation) [13], [14]. The enhancement of alite peak by sodium sulfate addition is seen in Fig 5a by comparing PL-30 NS with PL-30.

Fig. 5b shows the effect of SCMs on the early heat flow. All systems containing 30% PC exhibited a rather similar intensity of the alite peak (PL-30, PS-30, PLNp-30 and LC3-30). In contrast, LC3-50 showed a higher alite peak intensity compared to the previous systems, consistent with its greater PC content (50% versus 30%). Moving on to the aluminate peak, it can be seen that the systems containing MK displayed the greatest peak intensity, followed by S, Np, and L. It is worth mentioning that, despite having different PC contents, LC3-30 (1:1) and LC3-50 (2:1) have similar MK contents, which lead to aluminate peaks with comparable intensities. Overall, all (reactive) SCMs appear to contribute, to some extent, to the aluminate peak. For the materials in this study, this contribution follows the order: MK >> S > Np > L.

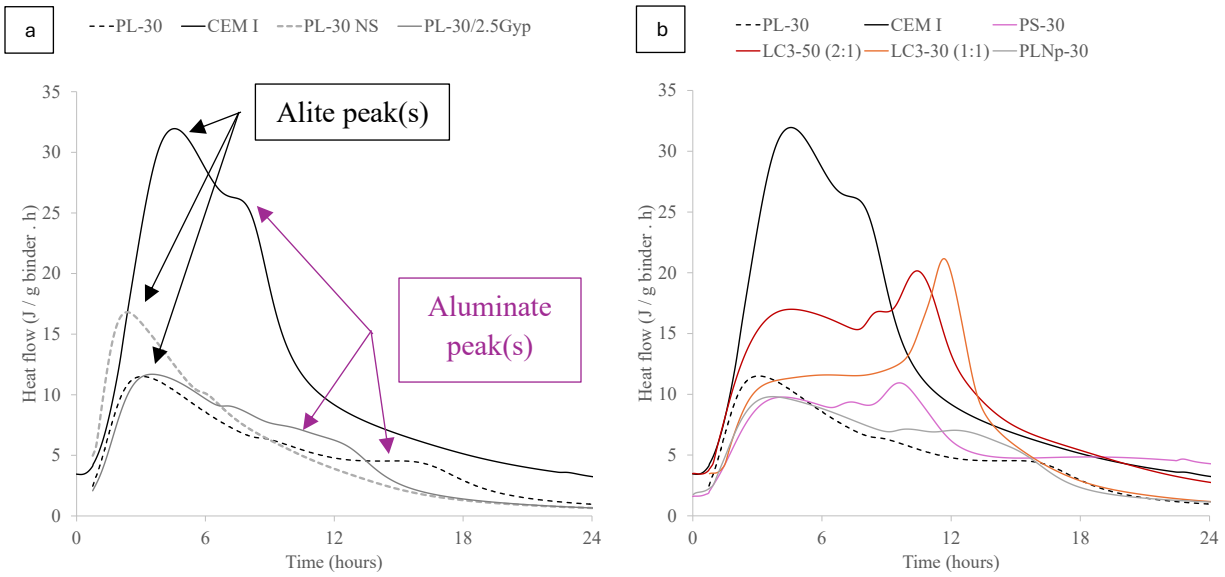
Although related, it is important to note that the effect on the aluminate peak should not be confused with the filler effect on the alite peak reported by [38], [39]. The latter appears to be primarily influenced by the fineness of the SCMs, with their reactivity being reported to play a secondary role [40].

Fig. 5c shows the effect of mineralized RFs on the early heat flow. All systems containing 30% PC exhibited a slightly higher alite peak intensity (compared to LC3-30 and PL-30). This effect may be consistent with the possibility that the filtration process after mineralization did not fully remove all alkali and sulfate ions used during mineralization. This hypothesis comes from the observation that the intensity of the alite peak of these mixes is in the same order or magnitude as for PC-NS in Fig. 5a. However, the effect mentioned before also fits the explanation of the early pozzolanic activity reported by [9], investigated via ^{27}Al and ^{29}Si magic-angle spinning nuclear magnetic resonance, which is considered a more reliable technique to study this specific effect.

Moving on to the aluminate peak, it can be seen that the system containing MK (LC3-30) still exhibited the highest peak intensity compared to the mineralized RFs, for which their contribution follows the order MK > M-LAB > M-Dcon > M-Dmix. The three different classes of mineralized materials clearly have distinct effects on the aluminate peak, which cannot be explained by the Al_2O_3 content obtained from XRF analysis or finenesses (Table 1), but appears to be consistent with the hydrated cement paste content measured by [17].

The type of waste used for mineralization may also influence the position of gypsum depletion valley. However, since the intensity of alite dissolution (and the adsorption of sulfates in C-S-H), as well as the remaining sulfate content in solution, significantly affect both the position of the aluminate peak and the onset of sulfate depletion, it is not appropriate to further discuss this aspect without strict control of the fineness of the RFs. This is particularly important given the inherent variability associated with materials derived from real waste streams.

Instead, a separate study using laboratory-prepared samples with well-defined cement paste contents and strictly controlled particle size distributions would be required in our view. Fig. S.3 also shows the effect of non-mineralized recycled fines on paste mixes.



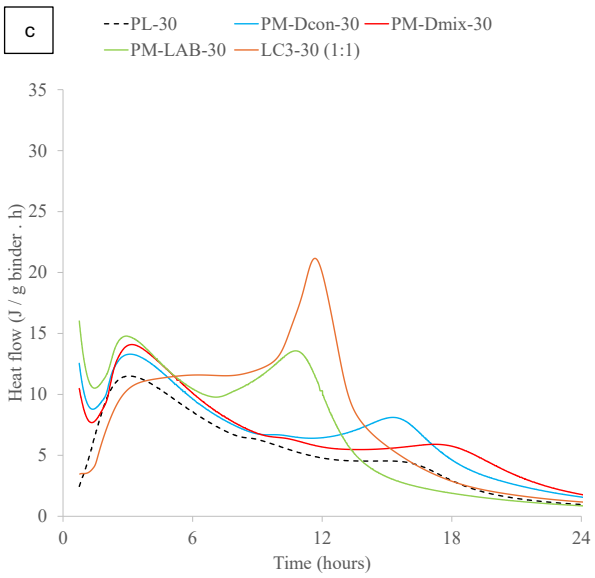


Figure 5. Heat flow during the first 24h obtained via isothermal calorimetry in systems a) CEM I and PC plus limestone (PL-30 and PL-30/2.5Gyp) with variable content of sulfate; b) CEM I, PL-30, PS-30, LC3-50 (2:1), LC3-30 (1:1) and PLNp-30 (1:1); and c) M-Dcon-30, M-Dmix-30 and M-LAB-30. Some systems are repeated in figures a-c to facilitate the visualization of the trends by the reader.

3.7. TGA on hydrated cement paste

Fig. 6a presents the calcium carbonate content for a selected group of samples from Table 2. A clear variation in $CaCO_3$ content is observed across the different formulations, consistent with the amount of limestone powder added in the mixes and the content of limestone presented in Table 4 for mineralized recycled materials. The highest values are recorded for PL-30 (approximately 71 g/100g) and PL-30NS (around 62 g/100g), indicating that the addition of sodium sulfate (for instance if the mineralized recycled fines are not carefully filtered) may have a measurable effect on the carbonate content. In contrast, PS-30 exhibits a very low $CaCO_3$ content, close to 3 g/100g, making necessary to account for the limestone content present in the mineralized recycled fines when comparing with traditional SCMs such as S or MK (in case of MK, only if not added in combination with limestone). In the specific case of the three mineralized RFs paste mixes in this study, the $CaCO_3$ content was 22 g/100g for PM-Dmix-30, 28 g/100g for PM-Dcon-30 and 35 g/100g for PM-LAB-30, which are in the same order of magnitude to LC3-30 (1:1) and PLNp-30 (1:1).

Fig. 6b shows the bound water and portlandite content calculated with tangential method (CH tg) of the mixes. BW is measured within the temperature range of 150–500 °C minus the bound water in CH tg. The range 150–500 °C is chosen to avoid errors caused by gypsum and AFm/AFt phases, which overlap in TGA curves, so they are difficult to separate and are not discussed here. Therefore, BW is only used as a rough indicator of how much the SCMs contribute to the formation of C-(A-)S-H within the range 150-500 °C.

All mixes with reactive SCMs [PM-Dcon-30, PM-Dmix-30, PM-LAB, LC3-30 (1:1) and PLNp-30 (1:1)] show BW values between about 6 and 8 g/100g of anhydrous binder. PS-30 shows higher BW values of

around 12 g/100g, which is because there is no dilution of slag with limestone filler, so there is more reactive material. The lowest BW is found in PL-30, which does not contain reactive SCMs. This mix can be used as a baseline for the contribution of the 30% PC to C-S-H formation. It is certainly important to note that the type of C-(A-)S-H formed in these mixes may differ because of aluminium incorporation, which is also known to change the amount of bound water per gram of C-(A-)S-H [22].

As expected, PL-30 and PL-30NS exhibited the highest portlandite contents (5.5–3.5 g/100g) due to the absence of pozzolanic materials. The remaining portlandite contents in M-Dcon, M-Dmix, M-LAB, MK, S, and Np were negligible when quantified using the tangential method. As previously discussed, the application of the stepwise method would result in an overestimation of the portlandite content (Fig. S.4, Supporting Information).

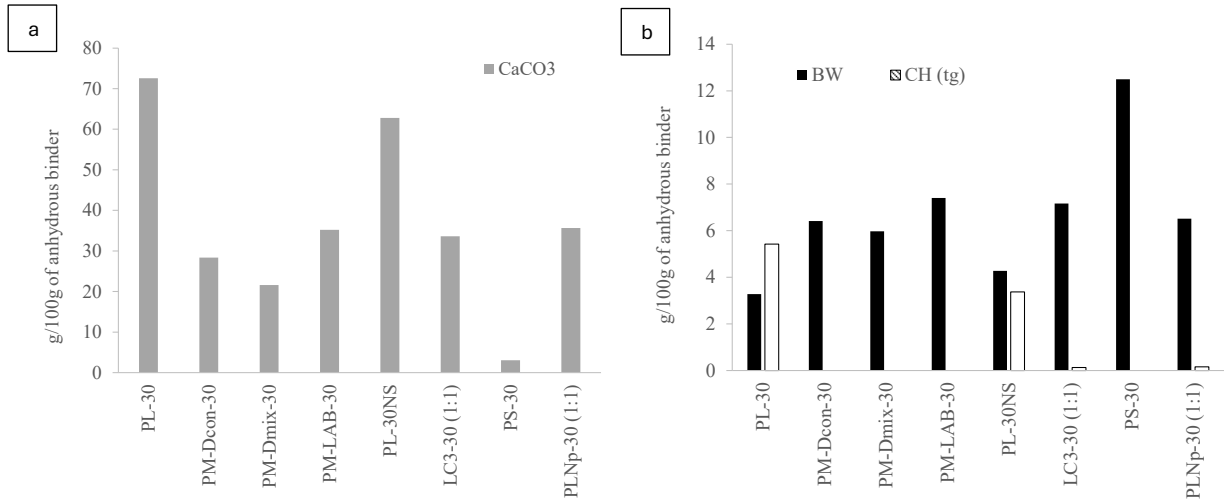


Figure 6. Quantification of a) carbonated calcium; and b) bound water (150-500 °C) excluding the contribution of portlandite, and portlandite content determined using the tangential method in cement paste systems.

3.8. Degree of reaction of SCMs in blended mixes

The DoR of the SCMs was estimated using two methods. The first method considers the amount of portlandite consumed in a given blended cement paste versus the amount of portlandite still available in the system containing a similar amount of PC blended with limestone filler which consumes limited portlandite. The amount of portlandite consumption is thus divided by the percentage of SCMs in such system and the portlandite that has been consumed by such SCM after modified R3 test. The second method considers the excess of heat release at a given age by the blended cement paste compared to the system containing a similar amount of PC blended with limestone filler. Such excess of heat is then divided by the percentage of SCMs in such system and the total heat released by such SCM at the end of the modified R3 test.

Fig. 7 shows the outcomes from the two methods. Both methods in fact point towards a degree of reaction in mineralized recycled fines (M-Dcon, M-Dmix and M-LAB) in the order of 40-to-50% when blended with 30%PC paste. Such values resulted similar to the 30-40% range measured for MK in LC3-30, higher

than for PS-30 in both cases. That is somehow expected given that the amount of reactive SCMs is larger in the PS-30 compared to all the other systems which contain a large amount of limestone in them. It is worth mentioning that (in theory) the DoR based on method 1 should not work well for the characterization of PS-30 because the unreacted slag particles could represent an additional source of calcium in the system and CH has been said to act merely an activator, instead of being consumed [41]. As also explained by [42], S activation requires to consume part of the existing portlandite reserve and reactions are then expected to be limited in this particular system by the availability of silica in the pore solution and effective precipitation of hydrates [13], [14], [43], possibly explaining the agreement between both methods. The DoR calculated for Np in PLNp-30 via isothermal calorimetry is also in the order of 40%.

The particular case of the DoR of Np in PLNp-30 deserves further attention, given the large discrepancy observed between the two methods. We believe this difference is related to the inability of the portlandite consumption approach to properly capture the actual phase assemblage developing in real systems (which is captured by calorimetry method). For example, the formation of 1 g of C-S-H with a Ca/Si ratio of 1.7 and S/H = 1 theoretically consumes approximately 0.39 g of Ca, whereas 1 g of C-A-S-H with a Ca/Si ratio of 1.2 and S/H = 1 consumes about 0.33 g of Ca. In contrast, the formation of 1 g of ettringite consumes only about 0.19 g of Ca. Consequently, for a similar amount of portlandite consumption, markedly different quantities of hydrates can be produced depending on the phase assemblage. Considering the densities of ettringite (≈1.75 g/cm³) and C-S-H with Ca/Si = 1.7 (≈2.6 g/cm³), the solid volume generated per unit of calcium consumed is approximately three times greater for ettringite than for C-S-H. Therefore, systems in which a larger fraction of the consumed calcium is incorporated into ettringite may exhibit substantially greater hydrate volumes despite similar levels of portlandite consumption, potentially leading to significant discrepancies depending on the method used to estimate DoR.

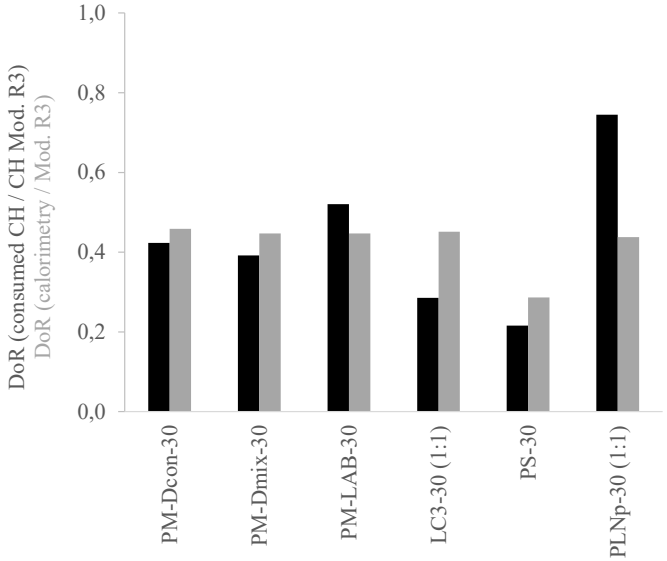


Figure 7. DoR of SCMs measured via CH consumption and excess of heat from isothermal calorimetry.

Despite being broadly used, both methods in this study have fundamental limitations. Their main advantages are their relative simplicity and the time savings they offer compared with more advanced characterization techniques such as SEM-BSE/EDS image analysis, ^{29}Si and ^{27}Al MAS NMR spectroscopy,

and quantitative XRD [44]. The main limitation of Method 1 is that its comparison to systems with higher PC contents becomes increasingly challenging because the calcium stored within the C-S-H structure cannot be captured by this approach (at similar PC content, the same initial calcium reserve is available and those differences are minimised). As a result, the DoR of the SCMs is expected to be systematically underestimated. As previously explained, it is neither possible to determine whether the consumed calcium is incorporated into AFt/AFm phases or into C-S-H. The proportion of calcium allocated to each of these phases would certainly affect the mechanical performance of the material, making it difficult to establish a direct relationship between calcium consumption and mechanical properties. Similarly, if the SCMs form a C-A-S-H phase with a lower Ca/Si ratio than that formed in the modified R3 solution, the potential amount of C-A-S-H formed may be considerably higher while the measured CH consumption remains unchanged. Therefore, this method would also fail to capture this important aspect of the hydration process [45].

Concerning Method 2, its principal limitation is the insufficient sensitivity of isothermal calorimetry for evaluating DoR at curing ages later than those considered in this study when conventional vials of approximately 20 cm^3 are used. After approximately 7 to 14 days, the measured heat flow approaches the level of the instrument's baseline noise, significantly reducing the signal-to-noise ratio and increasing the uncertainty associated with cumulative heat measurements [22]. Consequently, the determination of the extent of reaction becomes progressively less reliable over time. This limitation is particularly relevant because hydration reactions proceed at a substantially slower pace after the first week, leading to very low heat flow rates and only minor increments in cumulative heat release [44], [45].

3.9. Porosity assessment (MIP)

Table 5 presents the total porosity (%) of the paste samples after 7 days of curing at 40 °C, as measured by MIP (full intrusion curves are provided in Fig. S.1 and Fig. S.5 - supporting information). A reduction in clinker content has a pronounced effect on porosity, with lower clinker contents leading to a progressive increase in porosity. However, the total porosity of PS-30 is lower than that of LC3-50. This behavior can be attributed to the presence of significant reactive calcium oxide in the slag, which promotes additional hydrate formation despite the reduced clinker content, which is supported by the development of strength in following sections.

All samples (w/b=0.70) containing 30% PC showed very high total porosity values ranging from 67.2% (PL-30) to 53.5% (LC3-30). The differences between cement pastes prepared with mineralized and untreated recycled fines consistently fall within a relatively narrow range of 2.5–6.0 percentage points. For instance, in the case of PM-Dcon-30, the mineralization process reduced the porosity by approximately 5 percentage points compared to PDcon-30. Conversely, for M-LAB and MDmix systems, porosity slightly increased after mineralization.

The threshold pore size is defined as the pore diameter at which mercury begins to intrude significantly into the connected pore network. At larger pore diameters, pores are predominantly isolated; beyond this threshold, a continuous interconnected network becomes accessible. The results show that mineralization of RFs systematically decreases the threshold pore size in all cases. This is evident when comparing PM-Dcon-30, PM-Dmix-30, and PM-LAB-30 with their non-mineralized counterparts (PDcon-30, PDmix-30, and PLAB-30, respectively). Moreover, mixes incorporating mineralized RFs exhibit threshold pore sizes comparable to (or even smaller than) those of LC3-30, indicating a refinement of the pore network. The

threshold pore sizes for all samples follow the trend: PS-30 < CEM I < LC3-50 < PM-LAB-30 < PM-Dcon-30 < PM-Dmix-30 ≈ LC3-30 < PLAB-30 < PDmix-30 < PDcon-30 < PL-30.

Despite the values presented above, it is important to emphasize that the incorporation of (mineralized) RFs results in samples with high total porosity, which remains within the approximately 14 percentage points difference observed between PL-30 (inert filler) and LC3-30 (reactive MK). Porosity is influenced not only by the original recycled concrete source but also by the distinct effects induced by the mineralization process. The primary benefit of RF mineralization is not reflected in total porosity reduction, but rather in a significant refinement of the pore structure, as evidenced by the consistent decrease in threshold pore size when compared with PL-30. This indicates improved pore connectivity characteristics, even when the total porosity range measured via MIP does not substantially decrease.

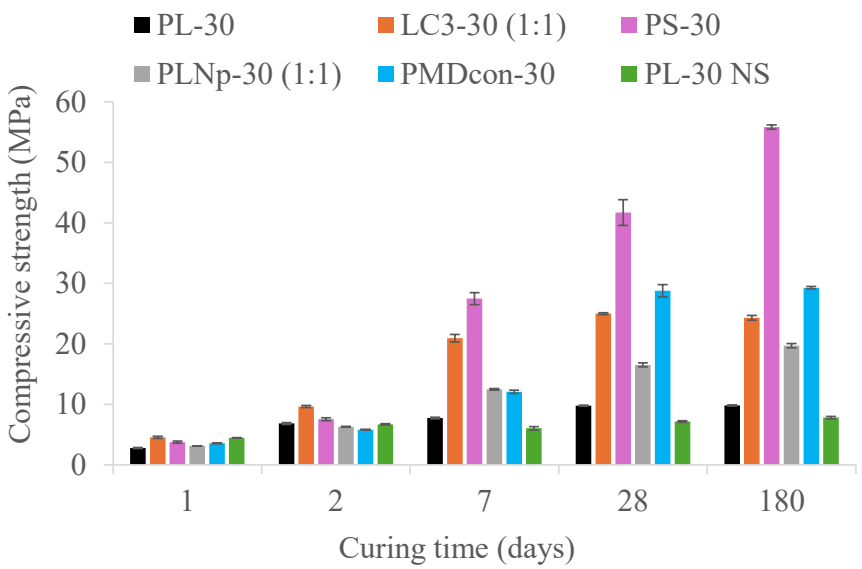
Furthermore, for applications where a specific porosity target is required (e.g., comparable to CEM I or LC3-50), the results suggest that adjusting the water-to-binder ratio (and possibly using superplasticizer) is a more effective strategy than relying on the selection of an optimal concrete waste source, which may be difficult to control in practice. This conclusion is supported by the trends observed in this section but also by the results obtained from paste samples made with variable w/b ratios in Fig. S.6. -supporting information file).

Table 5. Total porosity measured via MIP and threshold pore size. Error for porosity is estimated on ±2% from [13].

(W/B=0.70)	Total porosity (%)	Threshold pore size (nm)
PL-30	67,2	1576,8
PDcon-30	64,9	1235,6
PM-Dcon-30	59,1	580,0
PDmix-30	57,2	1090,9
PM-Dmix-30	59,7	618,7
PLAB-30	53,0	857,7
PM-LAB-30	57,1	408,0
CEM I	28,8	98,7
LC3-50	44,8	133,4
LC3-30	53,5	634,4
PS-30	40,4	35,7

3.10. Compressive strength and activity index.

Previous sections showed that our lab-made concrete might not fully reproduce the real behaviour of materials obtained from a real recycling plant flow stream (Dcon and Dmix) due to the marked presence of unreacted material. In addition, Dmix showed limited CO_2 capture capacity compared to Dcon, mainly due to the nature of the recycled fine content, which contains limited cement paste and more brick waste compared to Dcon [17]. Therefore, Dcon has been identified as the most promising material for mineralization and its potential use as an SCM in cement blends based on its reactivity (heat release and CH consumption) and CO_2 uptake potential. Thus, this section presents the strength contribution provided by M-Dcon when compared to traditional cement blends with 30% PC content.



642

643 Figure 8. Compressive strength evolution (1-180 days) for standard mortar samples from Table 3.

644 Fig. 8 shows the compressive strength development of PMDcon-30 compared to traditional SCMs such as
645 metakaolin, natural pozzolan, and slag. A blended cement incorporating PC and limestone was used to
646 account for the contribution of PC to strength (PL-30). All systems showed a similar strength at 1 day. LC3-
647 30 exhibited the highest strengths at 2 days. The slight differences in 2-day strength are associated with the
648 contributions provided by the SCMs, as previously evidenced by isothermal calorimetry (aluminate peaks).
649 Overall, all mixes exhibited strengths similar to those of the PL-30 mix (±3 MPa), indicating that the
650 contribution of the SCMs to strength development up to 2 days was rather limited.

651 The 7-day strength was highest for PS-30 cement, followed by the LC3-30, PLNp-30, and PMDcon-30
652 systems. Consistent with the observations of [46], the addition of extra alkalis to a PC-based system slightly
653 reduces the later-age strength, an effect that was already evident at 7 days. Consequently, PL-30 exhibited
654 slightly higher strength than PL-30 NS.

655 The 28-day strength was highest for PS-30, followed by the PMDcon-30 and LC3-30 systems. The PLNp-
656 30 mix showed some strength contribution (compared to PL-30) but remained approximately 10 MPa lower
657 than PMDcon-30. This trend remained the same at 180d. All systems containing pozzolanic materials
658 appeared to have a lack of calcium which is known to have a marked effect on sustaining the pozzolanic
659 reaction, as suggested by the results presented in the previous sections and the limited strength gain from
660 28 to 180 days. In contrast, when S was used, the system continued to gain strength due to the semi-
661 hydraulic reaction nature of the calcium-rich slag. Nevertheless, it was still observed that carbonated
662 recycled fines and calcined clays yielded higher strengths than the natural pozzolan. Even under calcium-
663 deficient conditions, the reactivity of the SCMs appears to correlate relatively well with their contribution
664 to compressive strength at 28 days, as shown in Fig. S.7 in the supporting information, and already
665 explained by [21] for a broader range of SCMs.

666 It should also be noted that PS-30 contains twice the amount of reactive SCMs compared to the other mixes;
667 therefore, its higher compressive strength at 28 and 180 days is due to both, greater calcium supply and
668 greater amount of reactive SCM. This mix aims to represent the strength development of a commercial

CEM III/B, a product well established on the market and used as a benchmark for recycled fines obtained through the mineralization of recycled concrete from a real recycling stream.

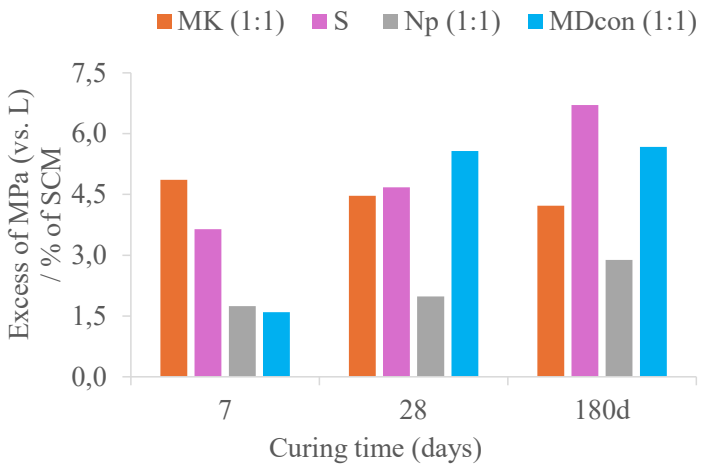


Figure 9. Activity indices of mortar mixtures incorporating MK, S, Np, and M-Dcon, measured after 7, 28 and 180 days of curing.

Fig. 9 shows the activity index for the mix in this study. The activity index counts the excess of compressive strength (in MPa) provided by the SCMs compared to a reference mix with the same content of PC but limestone filler instead (PL-30). However, such index alone would fail to account for the amount of filler added in the ternary mixes (LC3-30 for example). Therefore, the excess of strength is divided by the amount of reactive SCMs in the system (i.e., in the case of the slag, divided by 0.70 and in the case of MK (1:1), Np (1:1) and M-Dcon divided by 0.35).

Practically speaking there were no significant differences in the strength values measured at 1 and 2 days in Fig. 8, therefore activity index is only calculated for mixes at 7, 28 and 180 days of curing. MK and S are the SCMs that contribute the most to 7 day-strength. Np and M-Dcon show a contribution of half of the one provided by S and a third of the one provided by the MK, values that are in good agreement with the reactivity shown in Fig. 3. The contribution of MK remains rather stable at 28 and 180d, while it progressively increases for S and Np compared to 7 days. In case of M-Dcon, a significant increase is observed at 28 days, which is then mostly maintained at 180 days. The contribution of the Np remains the lowest, mainly associated with its limited R3 reactivity and known late pozzolanic reaction [47].

3.11. Environmental considerations

Fig. 10 presents the relationship between 28-day compressive strength and GWP/f_{c28}, where GWP/f_{c28} represents the global warming potential per unit compressive strength for 1 m^3 of mortar (kg CO_2 eq./MPa/m^3). Lower values on the horizontal axis indicate a more environmentally efficient material, as less CO_2 is emitted for each MPa of strength achieved by a m^3 of mortar.

The shaded green area highlights the region corresponding to relatively favorable performance, combining sufficient compressive strength for low load-bearing elements with low carbon intensity per unit strength.

The most desirable mixtures are located in the upper-left region of the graph, where compressive strength is high while GWP/fc28 remains low. Mixtures situated further to the right require a greater environmental burden to achieve a given strength level.

The CEM I marker exhibited the highest compressive strength, approximately 66 MPa, with a GWP/f_{c28} value of about 5.5 kg CO_2 eq./MPa/m^3. Mixes with LC3-50 showed improvements reaching GWP/f_{c28} values of about 4.0 kg CO_2 eq./MPa/m^3.

PS-30 reached a compressive strength of approximately 42 MPa with a GWP/f_{c28} ratio close to 5 kg CO_2 eq./MPa/m^3. PM-Dcon-30 and PM-Dcon-30* achieved strengths of about 29 MPa and exhibited relatively low GWP/f_{c28} values (approximately 3-4 kg CO_2 eq./MPa, depending on whether CO_2 uptake was considered), indicating good environmental efficiency but more limited mechanical performance.

The LC3-30 and PL-50 markers exhibited compressive strengths between approximately 25 and 27 MPa. These mixtures revealed environmental indicators comparable to higher-performing binders but with a lower strength. It is worth nothing that in many cases, the minimum binder content is limited by minimum content found in standards. Therefore, mixes with high filler contents could still show environmental benefits compared to CEM I when low strength applications are targeted.

PLNp-30 and PL-30 are located at approximately 7 and 12 kg CO_2 eq./MPa/m^3 and low compressive strength. These mixtures show both the lowest strength and the highest carbon intensity per unit strength, making it the least favorable option among those presented and highlighting the value of using more reactive SCMs (even in low strength low-clinker formulations).

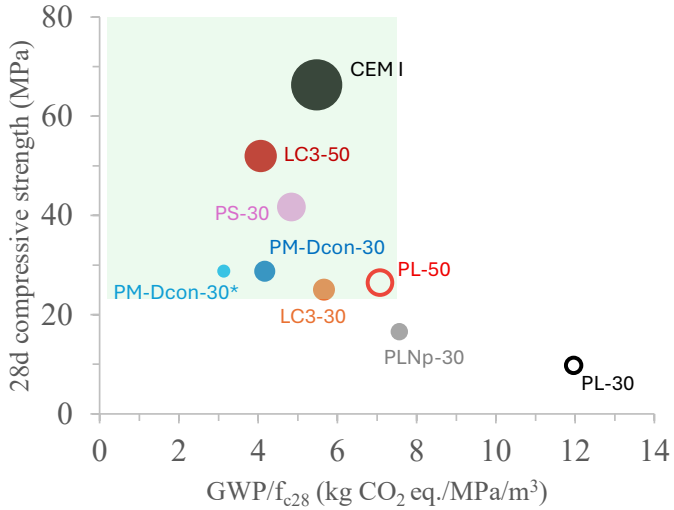


Figure 12. Plots of compressive strength vs. GWP per unit of compressive strength at 28 days (f_{c28}) for one cubic meter of mortar. Marker size provides an indication of the carbon footprint of each mortar mix, with larger markers representing higher kg CO_2-eq/m^3 of mortar. PM-Dcon-30* represents the scenario in which CO_2 uptake by M-Dcon is included in the carbon footprint calculations. CEM I, PL-50, and LC3-50 are reference mixes with w/b = 0.50, obtained from an unpublished study by the authors and included for

comparison with binders containing different clinker factors. The light green box highlights mixes that match or exceed the performance of PL-50 (50% PC, 50% limestone).

4. Conclusions

Applications in which moderate mechanical performance is the primary design criterion offer an opportunity to significantly reduce the clinker factor. In such low-clinker systems, which are characterized by calcium-deficient conditions, the efficient use of SCMs and their intrinsic reactivity become critical for developing sustainable formulations. This study evaluated the early-age performance of three CO_2-mineralized recycled fines (M-RFs) obtained from real waste streams as constituents of blended cements with clinker factors of approximately 30%, and benchmarked their performance against commercially available SCMs. Based on the results presented, the following conclusions can be drawn:

- The untreated recycled fines (Dcon, Dmix, and LAB) showed a limited contribution to early-age reactivity. Mineralization treatment accelerated heat release and portlandite consumption, as evidenced by both the modified R3 test and the ASTM-standard R3 test. This improvement was also observed in real low-clinker cement pastes containing M-Dcon, M-Dmix, and M-LAB. The main contribution to heat release occurred during the so-called aluminate peak. Although none of the mineralized recycled fines matched the contribution of metakaolin to the aluminate peak, they outperformed other SCMs, including natural pozzolan, limestone filler, and slag.
- Two methods were used to estimate the degree of reaction of the mineralized recycled fines in low-clinker systems. Both approaches yielded values of approximately 40% (after isothermal calorimetry), which were higher than those obtained for MK and slag in comparable systems.
- Bound water measurements between 150 and 500 °C were performed after isothermal calorimetry. After correcting for the contribution of portlandite, the MK, M-RF, and natural pozzolan systems showed similar amounts of chemically bound water. Furthermore, the calcium carbonate content measured in PM-Dcon-30 was comparable to that observed in the LC3-30 (1:1) system.
- Mercury intrusion porosimetry revealed a reduction in porosity for mixes containing M-RFs compared with those containing limestone filler. However, the main effect of mineralization was observed in the reduction of the threshold pore size, which reached values comparable to those of the LC3-30 (1:1) mix. The porosity of systems containing 30% PC was strongly influenced by the water-to-binder ratio, clinker factor, and drying conditions prior to testing, effects that exceeded the differences attributable to the SCMs evaluated in this study.
- Compressive strength and activity index results showed that M-Dcon achieved a performance comparable to that of natural pozzolan up to 7 days and slightly exceeded that of the LC3-30 (1:1) mix at 28 days. Nevertheless, none of the mixes containing pozzolanic materials reached the strength levels achieved by the laboratory-produced CEM III/B.
- The GWP per unit of compressive strength at 28 days for one cubic meter of mortar, positioned mixes containing M-Dcon favorably relative to the alternative SCM systems evaluated in this study, regardless of whether CO_2 uptake during mineralization was considered. Further improvements in 28-day compressive strength are still required for these systems to directly compete with available solutions such as CEM III/B.

The findings of this study represent a step forward towards the use of mineralized recycled fines derived from real waste-stream sources. They also highlight the importance of assessing not only the reduction in clinker content, but also whether such reductions translate into genuine environmental benefits while maintaining adequate mechanical performance. Certainly, a full LCA analysis is necessary to account for energy use during production of carbonated recycled fines at scale as well as possible CO_2 scaping production set-ups. However, we must emphasize that such process is perfectly suitable with renewable energies, therefore, it has the potential of being carbon 'neutral' since does not rely on fossil-fuel consumption. Follow-up studies will address these calculations at the scale of a production plant.

5. Acknowledgments

We would like to acknowledge Devagro Beton & Recyclage (Lars Rius and Krist Degezelle) for the fruitful discussions and Dr. Vadim Grigorjev for the support with the preparation of samples and characterisation of raw RFs. J.M.E acknowledges VLAIO IM (HBC.2025.0239) for the financial support.

6. References

[1] H. Van Damme, "Concrete material science: Past, present, and future innovations," *Cem. Concr. Res.*, vol. 112, no. January, pp. 5–24, 2018, doi: 10.1016/j.cemconres.2018.05.002.

[2] K. L. Scrivener, V. M. John, and E. M. Gartner, "Eco-efficient cements: Potential economically viable solutions for a low-CO2 cement-based materials industry," *Cem. Concr. Res.*, vol. 114, no. June, pp. 2–26, 2018, doi: 10.1016/j.cemconres.2018.03.015.

[3] CEMBUREAU, "CEMBUREAU key facts & figures," no. June, pp. 1–12, 2024, [Online]. Available: https://cembureau.eu/media/00ejjcfj/key-facts-figures-publication-june-2024.pdf

[4] R. Snellings, P. Suraneni, and J. Skibsted, "Future and emerging supplementary cementitious materials," *Cem. Concr. Res.*, vol. 171, no. May, 2023, doi: 10.1016/j.cemconres.2023.107199.

[5] "EUROSTAT, 2020. Waste statistics - Statistics Explained. https://ec.europa.eu/eurostat/statistics-explained/index.php?title=Waste_statistics#Data_sources (Accessed on 10/08/2026)."

[6] J. Moschen-Schimek, T. Kasper, and M. Huber-Humer, "Critical review of the recovery rates of construction and demolition waste in the European Union – An analysis of influencing factors in selected EU countries," *Waste Manag.*, vol. 167, no. May, pp. 150–164, 2023, doi: 10.1016/j.wasman.2023.05.020.

[7] M. Zajac, J. Skocek, P. Durdzinski, F. Bullerjahn, J. Skibsted, and M. Ben Haha, "Effect of carbonated cement paste on composite cement hydration and performance," *Cem. Concr. Res.*, vol. 134, no. April, p. 106090, 2020, doi: 10.1016/j.cemconres.2020.106090.

[8] M. Zajac, J. Skibsted, and M. Ben Haha, "Effect of alkalis on enforced carbonation of cement paste: Mechanism of reaction," *J. Am. Ceram. Soc.*, vol. 104, no. 2, pp. 1076–1087, 2021, doi: 10.1111/jace.17481.

[9] M. Zajac, J. Song, P. Ullrich, J. Skocek, M. Ben Haha, and J. Skibsted, "High early pozzolanic reactivity of alumina-silica gel: A study of the hydration of composite cements with carbonated recycled concrete paste," *Cem. Concr. Res.*, vol. 175, no. November 2023, 2024, doi: 10.1016/j.cemconres.2023.107345.

[10] M. Zajac, J. Skibsted, P. Durdzinski, and M. Ben Haha, “Effect of alkalis on products of enforced carbonation of cement paste,” *Constr. Build. Mater.*, vol. 291, p. 123203, 2021, doi: 10.1016/j.conbuildmat.2021.123203.

[11] M. Zajac, J. Skocek, J. Skibsted, and M. Ben Haha, “Co2 mineralization of demolished concrete wastes into a supplementary cementitious material – a new ccu approach for the cement industry,” *RILEM Tech. Lett.*, vol. 6, pp. 53–60, 2021, doi: 10.21809/rilemtechlett.2021.141.

[12] M. Zajac, J. Skibsted, B. Lothenbach, F. Bullerjahn, J. Skocek, and M. Ben Haha, “Effect of sulfate on CO2 binding efficiency of recycled alkaline materials,” *Cem. Concr. Res.*, vol. 157, no. April, 2022, doi: 10.1016/j.cemconres.2022.106804.

[13] J. M. Etcheverry, Y. A. Villagran-zaccardi, P. Van den Heede, V. Hallet, and N. De Belie, “Effect of sodium sulfate activation on the early age behaviour and microstructure development of hybrid cementitious systems containing Portland cement and blast furnace slag,” *Cem. Concr. Compos.*, vol. 141, no. December 2022, p. 105101, 2023, doi: 10.1016/j.cemconcomp.2023.105101.

[14] J. M. Etcheverry *et al.*, “Phase Evolution of Hybrid Alkali Sulfate-Activated Ground- Granulated Blast Furnace Slag Cements,” 2023, doi: 10.1021/acssuschemeng.3c05937.

[15] “Global decarbonization potential of CO2 mineralization in concrete materials,” 2024.

[16] P. P. Sivakumar, “Mix Development and Performance of Concrete with Treated Slag from Copper Production as Cement and Sand Replacement,” PhD thesis, Ghent University, 2022.

[17] V. Grigorjev, A. Laveglia, D. E. V. Madrid, V. Cnudde, M. Azenha, and N. De Belie, “Fine fractions of recycled aggregates: Integrated characterisation of physical and chemical properties, life cycle impacts and performance in cementitious mixtures,” *Constr. Build. Mater.*, vol. 518, no. January, p. 145829, 2026, doi: 10.1016/j.conbuildmat.2026.145829.

[18] M. Santhanam *et al.*, “RILEM TECHNICAL COMMITTEE RILEM TC-238 SCM recommendation on hydration stoppage by solvent exchange for the study of hydrate assemblages,” vol. 5, 2018, doi: 10.1617/s11527-018-1298-5.

[19] K. L. Scrivener, T. Matschei, F. Georget, P. Juilland, and A. K. Mohamed, “Advances in hydration and thermodynamics of cementitious systems,” *Cem. Concr. Res.*, vol. 174, no. September, p. 107332, 2023, doi: 10.1016/j.cemconres.2023.107332.

[20] P. Suraneni, A. Hajibabaee, S. Ramanathan, Y. Wang, and J. Weiss, “New insights from reactivity testing of supplementary cementitious materials,” *Cem. Concr. Compos.*, vol. 103, no. May, pp. 331–338, 2019, doi: 10.1016/j.cemconcomp.2019.05.017.

[21] D. Londono-zuluaga *et al.*, “Report of RILEM TC 267-TRM phase 3 : validation of the R 3 reactivity test across a wide range of materials,” vol. 3, 2022, doi: 10.1617/s11527-022-01947-3.

[22] K. Scrivener, R. Snellings, and B. Lothenbach, *A Practical Guide to Microstructural Analysis of Cementitious Materials*. 2018. doi: 10.1201/b19074.

[23] A. Laveglia, L. Sambataro, N. Ukrainczyk, N. De Belie, and E. Koenders, “Hydrated lime life-cycle assessment : Current and future scenarios in four EU countries BE IR,” *J. Clean. Prod.*, vol. 369, no. February, p. 133224, 2022, doi: 10.1016/j.jclepro.2022.133224.

[24] J. M. Etcheverry, A. Laveglia, Y. A. Villagran-Zaccardi, and N. De Belie, “A technical-environmental comparison of hybrid and blended slag cement-based recycled aggregate concrete tailored for optimal field performance,” *Dev. Built Environ.*, vol. 17, no. February, p. 100370, 2024, doi: 10.1016/j.dibe.2024.100370.

[25] R. G. Pillai *et al.*, “Cement and Concrete Research Service life and life cycle assessment of reinforced concrete systems with limestone calcined clay cement (LC3),” *Cem. Concr. Res.*, vol. 118, no. December 2018, pp. 111–119, 2019, doi: 10.1016/j.cemconres.2018.11.019.

[26] X. Chen, H. Wang, H. Najm, G. Venkiteela, and J. Hencken, “Evaluating engineering properties and environmental impact of pervious concrete with fly ash and slag,” *J. Clean. Prod.*, vol. 237, p. 117714, 2019, doi: 10.1016/j.jclepro.2019.117714.

[27] CEMBUREAU, “Key facts report 2024,” no. June, 2024, [Online]. Available: https://cembureau.eu/media/00ejjcfj/key-facts-figures-publication-june-2024.pdf

[28] Y. Hou, P. Y. Mahieux, P. Turcry, J. Lux, X. Jourdain, and A. Aït-Mokhtar, “Stockpile of recycled aggregates: A carbon sink?,” *Constr. Build. Mater.*, vol. 473, no. March, 2025, doi: 10.1016/j.conbuildmat.2025.140979.

[29] R. de Parisot, *Le projet national FastCarb a bénéficié du soutien financier du Ministère de la transition écologique et de la cohésion des territoires*. 2024. [Online]. Available: www.irex.asso.fr

[30] J. M. Etcheverry *et al.*, “Report of RILEM TC 281 - CCC : phase assemblage alterations and carbonation potential of mortar with blended cements induced by long duration carbonation exposure,” *Mater. Struct.*, 2025, doi: 10.1617/s11527-024-02555-z.

[31] P. Suraneni, A. Hajibabaee, S. Ramanathan, Y. Wang, and J. Weiss, “New insights from reactivity testing of supplementary cementitious materials,” *Cem. Concr. Compos.*, vol. 103, no. October 2018, pp. 331–338, 2019, doi: 10.1016/j.cemconcomp.2019.05.017.

[32] L. De Brabandere, V. Grigorjev, P. Van den Heede, H. Nachtergaele, K. Degezelle, and N. De Belie, “Using Fines from Recycled High-Quality Concrete as a Substitute for Cement,” *Sustain.*, vol. 17, no. 4, pp. 1–17, 2025, doi: 10.3390/su17041506.

[33] P. P. Sivakumar, Y. A. Villagrán-Zaccardi, T. Lapauw, E. Gruyaert, S. Matthys, and N. De Belie, “Durability Performance of Hybrid Binder Concretes Containing Non-Ferrous Slag and Recycled Aggregates,” *Sustain.*, vol. 15, no. 8, pp. 1–19, 2023, doi: 10.3390/su15086338.

[34] P. Suraneni, “Recent developments in reactivity testing of supplementary cementitious materials,” *RILEM Tech. Lett.*, vol. 6, pp. 131–139, 2021, doi: 10.21809/rilemtechlett.2021.150.

[35] M. Zajac, J. Skocek, P. Durdzinski, F. Bullerjahn, J. Skibsted, and M. Ben Haha, “Effect of carbonated cement paste on composite cement hydration and performance,” *Cem. Concr. Res.*, vol. 134, no. February, p. 106090, 2020, doi: 10.1016/j.cemconres.2020.106090.

[36] K. Scrivener, A. Ouzia, P. Juilland, and A. Kunhi Mohamed, “Advances in understanding cement hydration mechanisms,” *Cem. Concr. Res.*, vol. 124, no. July, p. 105823, 2019, doi: 10.1016/j.cemconres.2019.105823.

[37] F. Zunino and K. Scrivener, “Factors influencing the sulfate balance in pure phase C3S/C3A systems,” *Cem. Concr. Res.*, vol. 133, no. January, p. 106085, 2020, doi: 10.1016/j.cemconres.2020.106085.

[38] F. Zunino and K. Scrivener, “The influence of the filler effect on the sulfate requirement of blended cements,” *Cem. Concr. Res.*, vol. 126, no. August, p. 105918, 2019, doi: 10.1016/j.cemconres.2019.105918.

[39] A. Ouzia and K. Scrivener, “The needle model: A new model for the main hydration peak of alite,” *Cem. Concr. Res.*, vol. 115, no. August 2018, pp. 339–360, 2019, doi: 10.1016/j.cemconres.2018.08.005.

[40] F. Zunino and K. Scrivener, “Insights on the role of alumina content and the filler effect on the sulfate requirement of PC and blended cements,” *Cem. Concr. Res.*, vol. 160, no. July, p. 106929, 2022, doi: 10.1016/j.cemconres.2022.106929.

[41] E. Gruyaert, “Effect of blast-furnace slag as cement replacement on hydration, microstructure, strength and durability of concrete,” Ghent University, 2011.

[42] A. Parashar and S. Bishnoi, “Influence of the availability of calcium hydroxide, sulphates, and alkalis on hydration of supplementary cementitious materials,” *Cem. Concr. Res.*, vol. 175, no. November 2023, p. 107388, 2024, doi: 10.1016/j.cemconres.2023.107388.

[43] Y. Briki, M. Zajac, M. Ben Haha, and K. Scrivener, “Factors affecting the reactivity of slag at early and late ages,” *Cem. Concr. Res.*, vol. 150, no. September, p. 106604, 2021, doi: 10.1016/j.cemconres.2021.106604.

[44] K. L. Scrivener *et al.*, “TC 238-SCM: hydration and microstructure of concrete with SCMs: State of the art on methods to determine degree of reaction of SCMs,” *Mater. Struct. Constr.*, vol. 48, no. 4, pp. 835–862, 2015, doi: 10.1617/s11527-015-0527-4.

[45] P. T. Durdziński *et al.*, “Outcomes of the RILEM round robin on degree of reaction of slag and fly ash in blended cements,” *Mater. Struct. Constr.*, vol. 50, no. 2, 2017, doi: 10.1617/s11527-017-1002-1.

[46] M. Zhang, F. Zunino, L. Yang, F. Wang, and K. Scrivener, “Understanding the negative effects of alkalis on long-term strength of Portland cement,” *Cem. Concr. Res.*, vol. 174, no. October, p. 107348, 2023, doi: 10.1016/j.cemconres.2023.107348.

[47] J. M. Etcheverry, L. Detemmerman, K. Degezelle, V. Grigorjev, L. De Brabandere, and N. De Belie, “Durability Considerations in Replacing Blast Furnace Slag with Low-Grade Calcined Clay and Natural Pozzolan in Quaternary Cements,” pp. 1–23, 2025, doi: https://doi.org/10.3390/ma18215048.

7. Supporting information file:

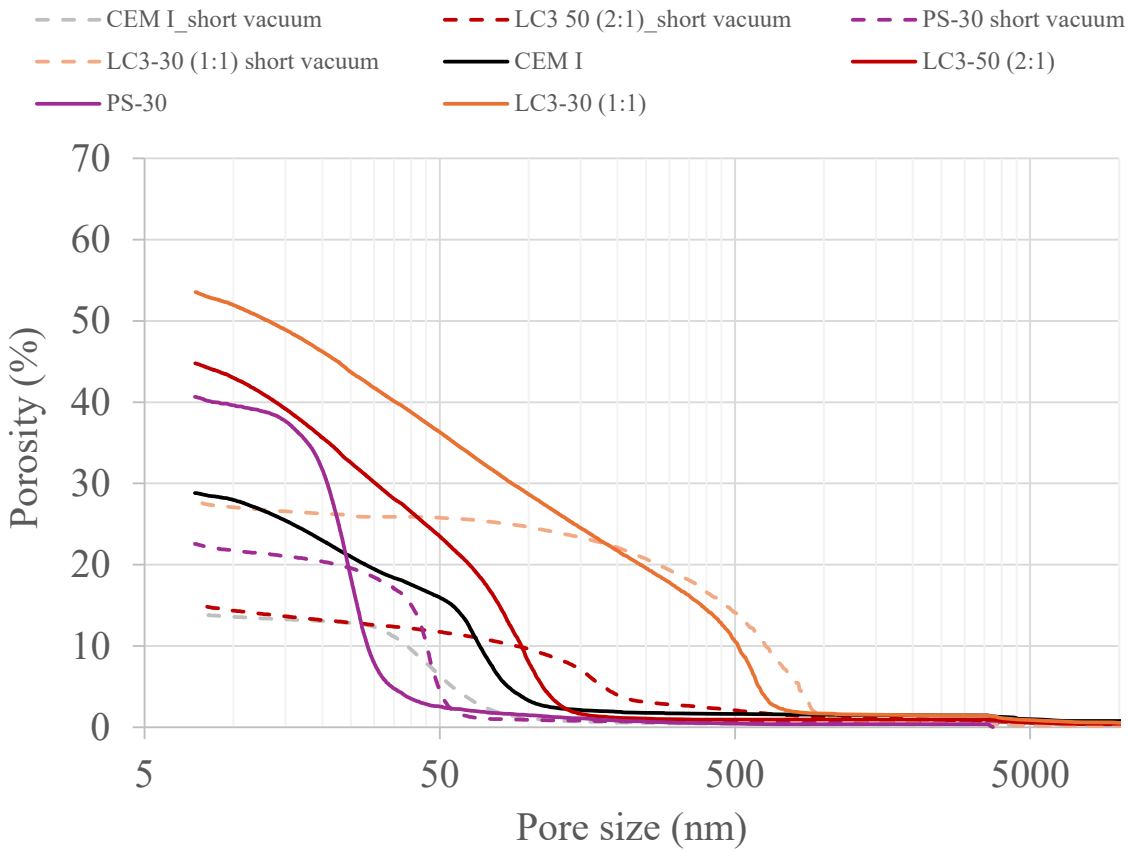


Figure S.1. Mercury intrusion porosimetry results showing self-desiccation effect in (blended) cements with vacuum drying of 2 days (short vacuum) and 1 month.

Table S.1. Burdens for calculations of kg of CO_2 eq. / m^3 of mortar.

Individual burdens (w/b=0.5)	kg CO_2 eq. /m^3 mortar
Sand	7,394
Mixing 1m^3	2,330
	kg CO2 eq. /kg material

PC	0,717
GGBFS Basic+econo. Alloc.	0,244
L	0,003
MK	0,149
Np	0,050
M-Dcon	0,018
M-Dcon with CO2 uptake	-0,070

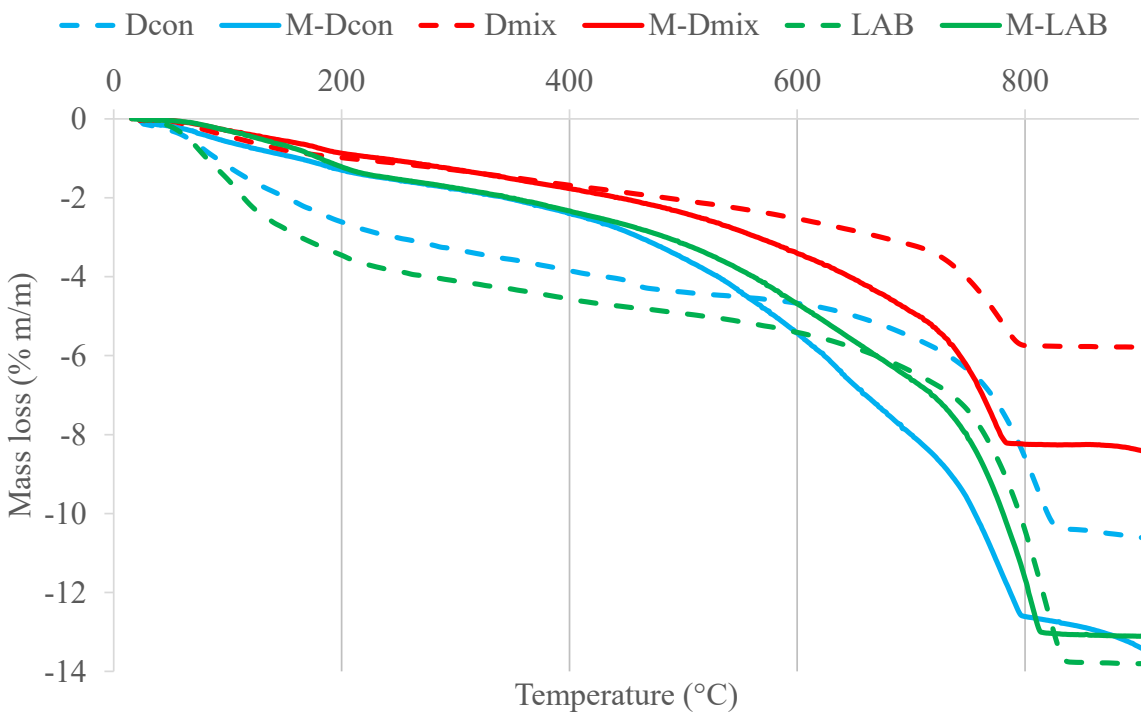


Figure S.2. Full TGA curve (20-900 °C) for recycled fines before mineralization and after mineralization (1h in 0.1M Na_2SO_4 solution + bubbling of 30% CO_2/ 70% N_2 at flow rate of 5 liters/h).

The pH (measured using a liquid to solid ratio = 5 and pH meter pre-calibrated with calibration solutions) of the non-mineralized mixes (~12.5±1.0) was found consistently higher than the one of the mineralized ones (~6.5±0.5). It can clearly be seen that the high pH of the non-mineralized RFs disturbs early cement hydration (Fig. S.3). A similar effect is commonly seen when adding

sodium hydroxide as activator. As a consequence, further sulfate adjustments would be necessary if these materials were meant to be used as filler.

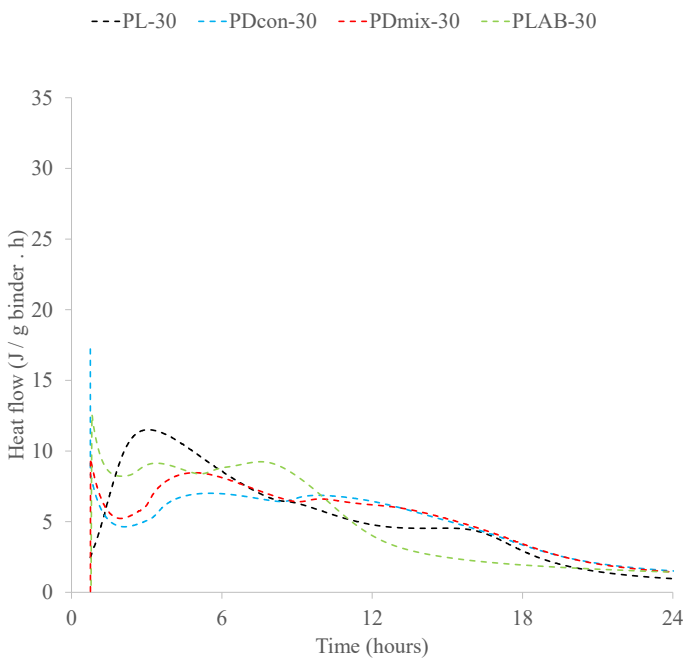


Figure S.3. Heat flow during the first 24h obtained via isothermal calorimetry in systems Dcon-30, Dmix-30, LAB-30 and PL-30.

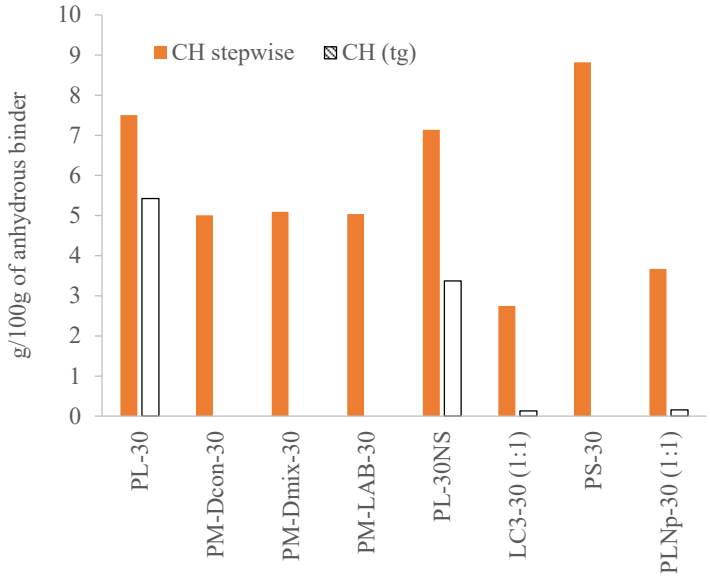


Figure S.4. Comparison of CH quantification using tangential and stepwise methods. The stepwise method leads to a clear overestimation of the CH content.

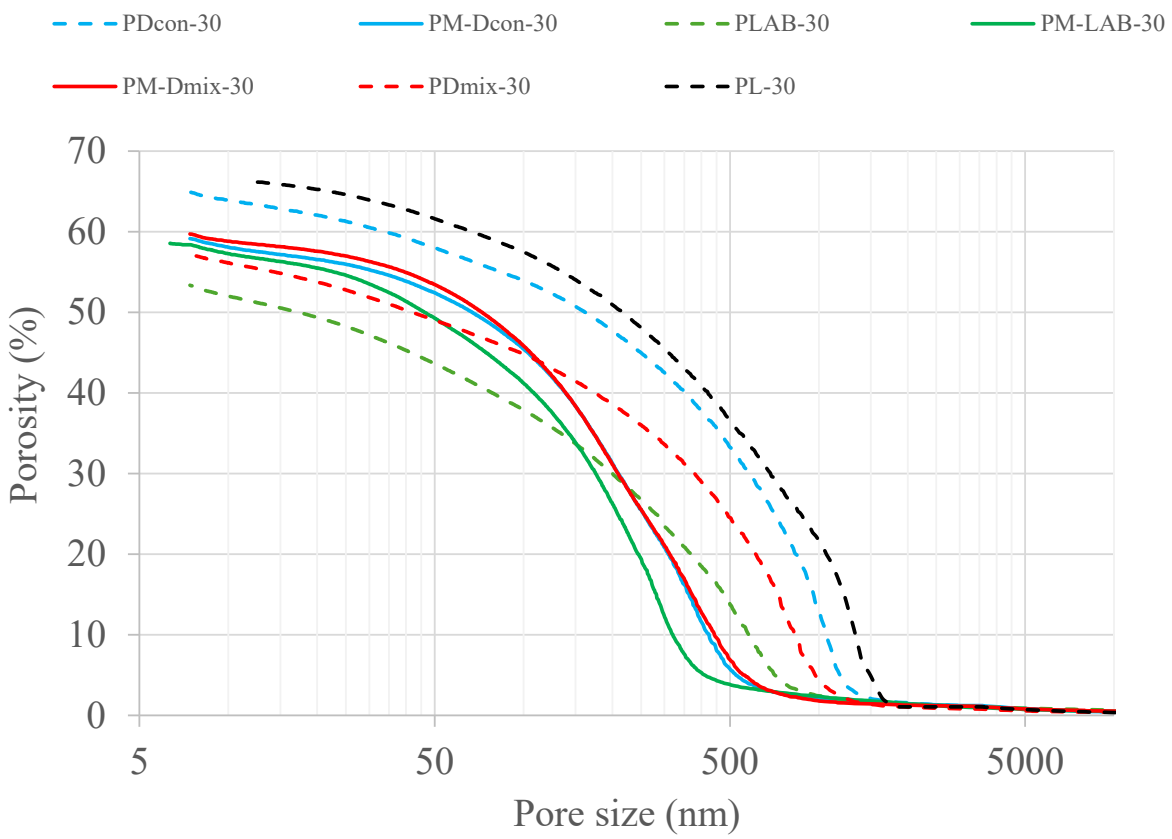


Figure S.5. Porosity versus pore size obtained via MIP on (non-) mineralized recycled fines paste samples and PL-30.

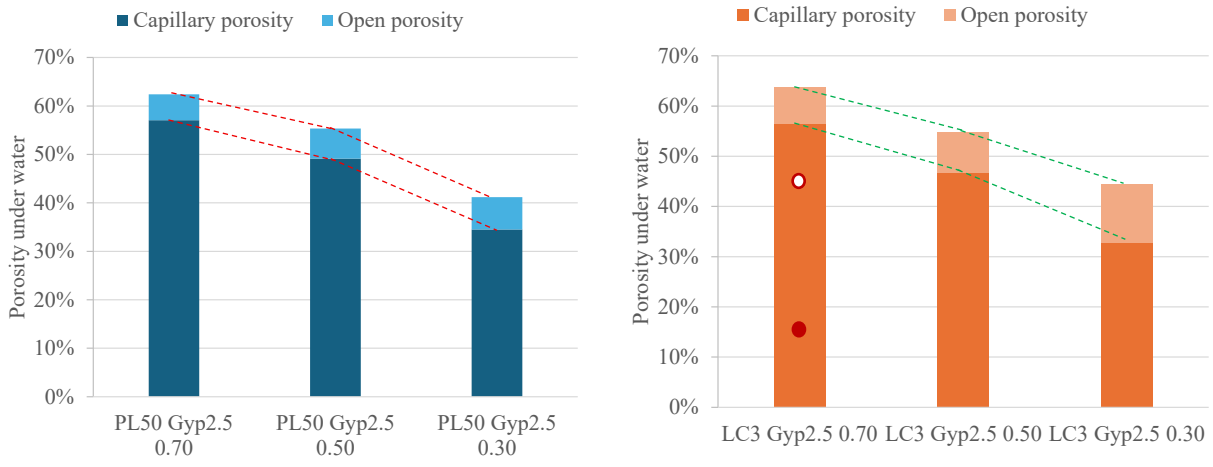


Figure S.6. Porosity under vacuum measured on paste sample at water-to-binder ratios 0.70, 0.50 and 0.30 for PL-50 (50% PC + 50% L) and b) LC3-50 (2:1). The white and red dots represent the values measured via MIP (vacuum dried sample for 1 month and 1 day, respectively).

Fig. S.6 shows that the variations in (capillary and open) porosity measured with porosity under vacuum at water-to-binder ratios 0.70, 0.50 and 0.30 for PL-50 and LC3-50 (2:1). Limited differences are observed in the values of porosity of LC3-50 (2:1) and PL-50 by this technique at the same water to binder ratio. In addition, the comparison of the results for LC3-50 0.70 in Fig. S.6 and LC3-50 in Fig. S.1 (MIP) reveals that the porosity measure via MIP results naturally lower than the one measured via porosity under vacuum. The main reason is that MIP only measures the porosity within a limited pore size range.

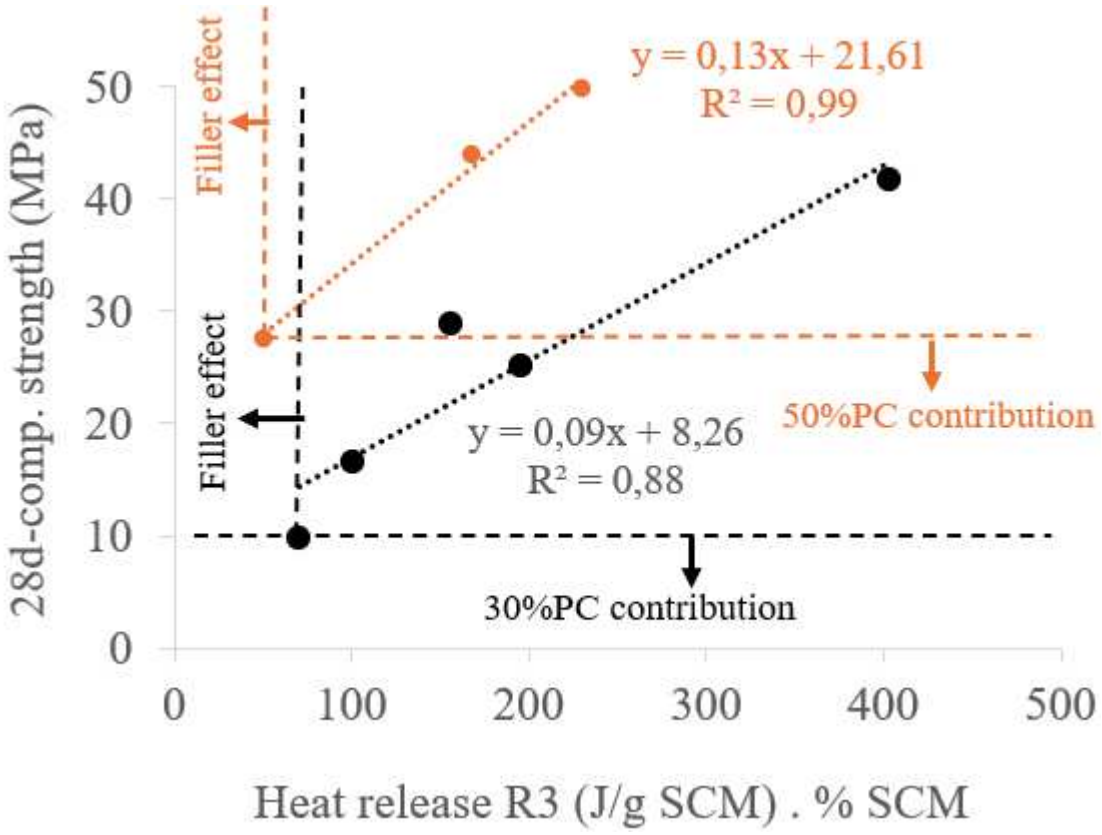


Figure S.7. Correlation between 28 days compressive strength and heat release by SCMs and limestone filler in R3 test, multiplied by the corresponding amount of reactive SCM and filler in the cement blend. In black, systems containing 30% PC and in orange, systems containing 50% PC (from left to right; 50%PC-50%L, 50%PC-30%MK-15%LL-5%gyp and 50%PC-45%MK-5%gyp).